ON THE BEHAVIOR OF SYMMETRIC WAVES IN STRATIFIED SHEAR LAYERS

BY JØRGEN HOLMBOE

FREMLAGT I VIDENSKAPS-AKADEMIETS MØTE DEN 9DE FEBRUAR 1962

Summary. The physical mechanism of hydrodynamical instability is examined in cases where an upper warm layer of air is moving relative to a lower cold layer. The two layers are separated by a shear layer where the wind has a continuous variation with height. Three models with different distribution of temperature in the shear layer are considered, namely: (i) The entire temperature change is located at the center of the shear layer, in chapter I. (ii) The shear layer has a constant potential temperature equal to the arithmetic mean of the outer temperatures, in chapter II. (iii) The wind shear and temperature stratification have continuous (hyperbolic tangent) variations in the shear layer, in chapter III. The results represent generalisations of earlier results by HELMHOLTZ, RAYLEIGH, TAYLOR and GOLDSTEIN: The model (i) has overstability, that is oscillations with growing amplitudes, in a spectral band which shifts toward shorter waves with increasing static stability. The kinematic structure and overstable growth mechanism of these waves are discussed in section 9. This system has no neutral waves which are stationary with reference to the air at the central temperature interface. The transition waves from stability to overstability perform stable oscillations with no growth rate. The model (ii) has instability, that is stationary wave-tilt with exponential growth, in a spectral band which shifts toward shorter waves with increasing static stability. The transition waves from stability to instability are non-tilting neutral waves which are stationary relative to the air at the center of the shear layer. These transition waves have a very simple structure (section 12) which gives the key to the interpretation of the growth mechanism of the unstable waves (section 16). The model (iii) has stationary neutral waves which are similar in kinematic structure to the transition waves in the discontinuous model (ii). However the waves are significantly different near the center of the shear layer and their behavior is accounted for by this difference. It is possible to construct quasi-stationary waves in model (iii) which are quite similar in all respects to the transition waves in model (ii).

Professor VILHELM BJERKNES' famous circulation theorem in 1898 opened the door to the physical hydronynamics of large scale baroclinic motions in the atmosphere. The following article is an attempt to extend some of Bjerknes' ideas in a limited area of this field of science. It is the author's hope that it may reflect a little of the inspiration that he received in his youth under the influence and guidance of his great teacher and benefactor.

LIST OF CONTENTS

1. Introduction. The stability of a fluid layer in which the density and velocity vary with height was examined by G. I. Taylor in 1914, but he delayed publication of his results until 1931 [1] when the same problem was studied by S. Goldstein [2]. Both investigations were carried out by assuming disturbances in the form of progressive waves moving in the direction of the basic flow, the so-called *normal modes* of the system. Taylor makes the following comment in the introduction to his paper: "It is a simple matter to work out the equations which must be satisfied by waves in such fluids, but the interpretation of the solutions of these equations is a matter of considerable difficulty".

In the present work an attempt is made to avoid some of these difficulties by using a different method of analysis: GOLDSTEIN noted that the equations are simplified if the total change in density from the bottom to the top of the shear layer is a small fraction of the mean density. In that case the kinematic asymmetry due to the different inertia of the upper and lower layers may be ignored without losing the basic dynamic characteristics of the systems. If further the wind shear and the stratification of mass are symmetric with reference to some central level, the shear layer has both kinematic and dynamic symmetry with reference to that level in a frame of reference which moves with the fluid at that level. We shall call such systems symmetric shear layers, and the frame which moves with the fluid at the central level is called the *symmetric frame*.

The usual method for examining the stability of a hydrodynamical system is to look for the spectrum of normal modes of the system. These are small amplitude sine waves whose evolution in time is simple harmonic. If any of the modes tend to grow exponentially with time, the same is true for an arbitrary local disturbance which according to Fourier must contain the unstable mode in its spectrum. The system is in that case regarded as unstable. But this method does not give a clear physical idea of the wave mechanism. The normal modes propagate with the same speed at all levels regardless of the wind profile of the basic flow. This means that the modes propagate with different speeds *through the air*. Because of this constraint the normal modes have in general an asymmetric structure along the vertical. If the shear layer is quasi-symmetric the normal modes do not reflect the basic dynamic symmetry of the layer in a simple manner. The dynamic characteristics of the layer are better understood by examining the behavior of wave disturbances which have the same vertical symmetry as the basic flow. These symmetric waves have the same behavior in the upper and lower part of the shear layer. The dynamic symmetry of the system assures the continued symmetry of the wave at all times.

The vertically symmetric waves, in their evolution of growth and decay, reveal rather clearly the physical processes which modify the waves. Moreover the symmetric waves in a central layer of *constant shear* are rather similar in structure to the simplest solutions in shear layers with continuous variation of stratification and shear, so they are helpful for the interpretation of these solutions.

The theory of symmetric waves is of course closely related to the theory of normal modes. The growing and decaying modes are obtained very simply as a special case from the symmetric wave theory, and the neutral modes are obtained as a linear combination of symmetric waves. Conversely the symmetric waves may be obtained by a linear combination of one or several pairs of normal modes. The symmetric theory can be recovered from the normal mode theory and vice versa. The two methods are mathematically equivalent, representing different linearly independent sets of solutions of the basic wave equations.

2. The constant shear layer. Consider first a central layer of constant shear between irrotational outer layers of equal depth. In the symmetric frame the air in the outer layers moves in opposite directions with the same speed U. The shear layer has the depth d, so the air in the shear layer has constant vorticity of magnitude

$$q = 2U/d. \qquad \text{(Shear layer vorticity).} \tag{2.1}$$

The outer layers each have a constant potential temperature with the warmer air ($\theta = \theta_w$) above and the colder air ($\theta = \theta_c$) below the shear layer. The static stability of the shear layer is measured by the non-dimensional parameter

$$s = {}^1/_2(\theta_w - \theta_c)/(\theta_w + \theta_c) \ll 1. \quad \text{(Quasi-symmetry condition).} \tag{2.2}$$

The dynamic behavior of the quasi-symmetric shear layer is governed by a non-dimensional Richardson Number, namely

$$\mu = sgd/U^2. \tag{2.3}$$

It remains to specify the temperature (or mass) distribution within the shear layer. The most satisfactory model would be one with continuous variation of potential temperature from θ_c at the bottom to θ_w at the top of the shear layer. Such a model has been examined by GOLDSTEIN [2] and several others. In order to develop tools for the interpretation of the wave solutions in model with continuous mass-distribution, we shall first consider two limiting models with a very simple discontinuous mass distribution:

(i) The entire temperature change $\theta_c \to \theta_w$ is located at the central level of the shear layer. Above and below this sharp temperature interface the air in the shear layer has the same potential temperature as in the adjoining outer layers. This model with unbounded outer layers will be examined in Chapter I.

(ii) The shear layer has a constant potential temperature equal to the arithmetic mean of the outer temperatures. This model with outer layers of finite depth will be treated in Chapter II. TAYLOR and GOLDSTEIN examined this model with unbounded outer layers.

A special shear layer model with continous distribution of temperature and shear will finally be discussed briefly in Chapter III.

3. The vorticity fields of a wave in a symmetric constant shear layer. The vorticity field of a wave disturbance in a constant shear layer and its changes are governed by two distinct physical processes, one kinematic and one dynamic process. The wave-mechanism is better understood if one keeps track of these two separate parts of the total vorticity budget of the wave.

(i) *The kinematic vorticity wave.* This part is associated with the deformations of the boundaries of the shear layer and the corresponding redistribution of the constant vorticity of the air in the shear layer. Let any one of the two boundaries be given a small-amplitude sinusoidal deformation with the wave length $L = 2\pi/k$, such that the air particles in the boundary have vertical displacements of the form

$$z_s = A_s \cos kx. \qquad (A_s k \ll 1). \tag{3.1}$$

This deformation of the boundary gives rise to a sinusoidal field of vorticity, the constant vorticity of the shear layer having been added in the sinusoidal segments outside the boundary level and removed from the segments inside the boundary level. This added vorticity field is associated with a Laplacean velocity field in the surrounding air. The change of the tangential component of this Laplacean field across the sinusoidal segment of added vorticity is according to Stoke's Theorem and (2.1)

$$(u^+ - u^-)_s = \pm\, q z_s = \pm\, (2U/d) z_s. \tag{3.2}$$

If the intrinsic propagation of the wave through the air is much slower than the speed of sound (the usual case for shear layers of practical interest), the compressibility of the air may be ignored, and the velocity field is quasi-solenoidal. Let the component velocity field in (3.2) be denoted by the vector $\boldsymbol{v}$. The corresponding stream-function ψ of this field may be assigned such that

$$\boldsymbol{v} = u\boldsymbol{i} + w\boldsymbol{k} = \nabla \psi \times \boldsymbol{j}. \tag{3.3}$$

Here $\boldsymbol{i}, \boldsymbol{j}, \boldsymbol{k}$ is the right handed orthogonal triple of unit vectors of a rectangular frame of reference (x, y, z) with $\boldsymbol{i}$ along the direction of the flow in the upper layer, $\boldsymbol{k}$ along the positive vertical, and $\boldsymbol{j}$ along the vorticity in the shear layer. When the outer layers are unbounded, the streamfunction of the field associated with the sinusoidal distribution of kinematic vorticities (3.2) has the form

$$\psi = \psi_s e^{-k|z|}, \text{ so } (u^+ - u^-)_s = 2k\psi_s, \tag{3.4}$$

where ψ_s denotes the streamfunction value along the boundary level and z is measured from that level. The kinematic vorticities (3.2) at the boundaries of the shear layer accordingly give rise to Laplacean component fields whose streamfunctions have the boundary level values,

$$\psi_s = \pm\, (U/\varkappa) z_s. \qquad (\varkappa = kd) \tag{3.5}$$

The positive sign applies to the upper boundary and the negative sign applies to the lower boundary. If only one boundary is deformed, the field associated with the corresponding local kinematic vorticities would propagate this deformation upwind as an instantaneously neutral wave with the phase velocity $U/\varkappa$.

(ii) *The dynamic vorticity wave.* Besides the kinematic vorticities at the shear layer boundaries the wave has in general sliding vorticities along the interfaces where the temperature (or density) undergoes an abrupt change. The model (i) has one such interface at the central level. The model (ii) has two such interfaces coincident with the boundaries of the shear layer. While the kinematic vorticities are permanently conserved on the air particles in the shear layer, the sliding vorticities along the density discontinuities are continually changed by the static stability (overweight) of the interface particles. The sliding vorticity acceleration is determined by the vorticity equation for the interface particles (the dynamic boundary conditions). For a quasi-symmetric system this equation has, in HØILAND's formulation [3], the simple form

$$\frac{D}{Dt}(u^+ - u^-)_T = 2Sg\frac{\partial z_T}{\partial x}, \quad \text{(Dynamic boundary condition)}$$

where z_T denotes the deformation of the temperature discontinuity and S has the value s in (2.2) at the boundaries of the shear layer in model (ii) and S has the value $2s$ at the central interface in model (i). The sliding vorticities across the temperature interfaces are the only vorticities subjected to these dynamic changes. To distinguish them from the kinematic vorticities we shall call them the dynamic vorticities of the wave.

Precisely as the kinematic vorticities in (3.2) the dynamic sliding vorticities give rise to Laplacean velocity fields in the surrounding air whose streamfunction value ψ_T at the interface level, as in (3.4), is given by

$$(u^+ - u^-)_T = 2k\psi_T.$$

With this value of the sliding vorticity substituted, the dynamic boundary condition becomes

$$\frac{D\psi_T}{Dt} = Sgd\frac{\partial}{\partial x}\left(\frac{z_T}{\varkappa}\right) \qquad (\varkappa = kd). \tag{3.6}$$

This equation gives the evolution of the dynamic vorticity wave at every temperature interface when its deformation z_T is known. The evolution of the vorticity wave is determined by the local conditions at the interface, and it is independent of conditions elsewhere.

On the contrary the evolution of the interface deformations are determined by the entire velocity field. The interfaces are moved by all the component fields associated with the kinematic vorticities and the dynamic vortisities in the wave.

CHAPTER I

SHEAR LAYER WITH STATIC STABILITY ACROSS THE CENTER LEVEL. (MODEL I)

4. Symmetric waves in a constant shear layer with a temperature discontinuity in the middle. Let z_1 and z_2 denote the deformations of the upper and lower boundary of the shear layer, and let z_T denote the deformation of the central temperature interface. Let ψ_T denote the center level streamfunction value of the component velocity field which is associated with the dynamic sliding vorticities $(u^+ - u^-)_T$ across this interface. An arbitrary symmetric wave in this system has the wave elements

$$
\begin{aligned}
z_1 &= A_s\cos(kx - \sigma) = \xi \cos kx + \eta \sin kx, \\
-z_2 &= A_s\cos(kx + \sigma) = \xi \cos kx - \eta \sin kx, \\
z_T &= A_T\sin kx; \qquad \psi_T = \frac{U}{\varkappa}A \cos kx \qquad (\varkappa = kd).
\end{aligned}
\tag{4.1}
$$

The amplitude A of the dynamic vorticity field has been chosen in such a way that the ratio between this vorticity and the kinematic vorticity at the boundaries of the shear layer (see 3.5) is equal to the amplitude ratio A/A_s. The dynamic symmetry of the shear layer assures the symmetry of the wave in (4.1) at all times, so the amplitudes A_s, A_T, A and the phase σ are functions of time only.

Let us represent the evolution equations for the wave in (4.1) non-dimensionally by using units of length and time such that $U = k = 1$. We have earlier introduced the non-dimensional Richardson Number μ in (2.3) which depends upon the stability parameter s in (2.2). In the present model the stability parameter S in the dynamic vorticity equation (3.6) has the value $2s$. We now introduce the additional non-dimensional parameters

$$
\begin{aligned}
n_s^2 &= \frac{Sgd}{\varkappa U^2} = \frac{2\mu}{\varkappa} \\
a &= e^{-\varkappa} \qquad (\varkappa = kd)
\end{aligned}
\tag{4.2}
$$

In the symmetric frame of reference which moves with the air at the central level the dynamic vorticity condition (3.6) and the kinematic condition at the central temperature interface are

$$
\begin{aligned}
\frac{\partial \psi_T}{\partial t} &= n_s^2 \frac{\partial z_T}{\partial x} \\
\frac{\partial z_T}{\partial t} &= \frac{\partial}{\partial x}\left[\psi_T + \frac{\sqrt{a}}{\varkappa}(z_1 - z_2)\right].
\end{aligned}
\tag{4.3}
$$

The kinematic condition states that the central interface is moved by the dynamic vorticity field ψ_T and by the two kinematic vorticity fields, $\pm z_s/\varkappa$ (see 3.5) at the boundaries of the shear layer which are reduced by the factor $\sqrt{a} = \exp(-{}^1/_2\, kd)$ at the central level. The kinematic conditions at the boundaries of the shear layer are

$$\left(\frac{\partial}{\partial t} + \frac{\partial}{\partial x}\right) z_1 = \frac{\partial}{\partial x}\left(\frac{z_1}{\varkappa} - a\,\frac{z_2}{\varkappa} + \sqrt{a}\psi_T\right), \tag{4.4}$$

$$\left(\frac{\partial}{\partial t} - \frac{\partial}{\partial x}\right) z_2 = \frac{\partial}{\partial x}\left(a\,\frac{z_1}{\varkappa} - \frac{z_2}{\varkappa} + \sqrt{a}\psi_T\right).$$

Before we examine the general solutions of this system of equations it will be useful to consider two special cases, namely: (i) an unbounded shear layer and (ii) an isentropic (homogeneous) shear layer.

5. The unbounded shear layer ($d \to \infty$). The kinematic conditions (4.4) for the boundaries of the shear layer are here of no consequence. The boundary conditions for the central temperature interface in (4.3) reduce to those of a simple gravity wave, namely

$$\frac{\partial \psi_T}{\partial t} = \left(\frac{n_s}{k}\right)^2 \frac{\partial z_T}{\partial x}\,; \quad \frac{\partial z_T}{\partial t} = \frac{\partial \psi_T}{\partial x}. \qquad (n_s^2 = Sgk) \tag{5.1}$$

The symmetric wave in (4.1) performs the standing gravity oscillations

$$z_T = A_T \sin kx \cos n_s t, \quad \psi_T = (n_s/k) A_T \cos kx \sin n_s t, \tag{5.2}$$

with the gravitational frequency n_s in (5.1). The symmetric wave is here identical to the normal mode of the system.

6. The isentropic shear layer ($s \to 0$). This system cannot develop dynamic sliding vorticities at the central level so the conditions (4.3) have no meaning, while the kinematic conditions in (4.4) reduce to those of simple kinematic vorticity waves in the boundaries of the isentropic shear layer. These waves were first examined by Lord Rayleigh [4]. It will be helpful for the later discussions to review the theory of the Rayleigh waves very briefly. The difference and sum of the kinematic conditions (4.4) for the symmetric Rayleigh wave in (4.1) are

$$\dot{\xi} = (1 - n_a)\eta, \qquad n_a \equiv (1 - a)/\varkappa, \tag{6.1}$$

$$\dot{\eta} = (1 - n_b)\xi. \qquad n_b \equiv (1 + a)/\varkappa.$$

When either η or ξ are eliminated, we see that both obey the same simple harmonic equation,

$$\ddot{\xi} = -n_R^2 \xi. \qquad n_R^2 \equiv (1 - n_a)(1 - n_b). \tag{6.2}$$

We shall call the non-tilting state of the symmetric wave with the boundaries deformed in phase ($\sigma = 90°$) the *a-state* of the wave. The second non-tilting state with the boundaries deformed in opposite phase ($\sigma = 0$) will be called the *b-state* of the wave.

Starting from an initial b-state with the interface amplitude $A_s = A_b$, the symmetric Rayleigh wave has the evolution:

$$\xi = A_s \cos \sigma = A_b \cos n_R\, t, \qquad \eta = A_s \sin \sigma = (1 - n_b)\, A_b \sin n_R t / n_R. \tag{6.3}$$

In particular the phase of the wave has the evolution

$$\tan \sigma = (1 - n_b) \tan n_R t / n_R. \tag{6.4}$$

In an arbitrary state (A_s, σ) the upper and lower component waves have both the same *downwind* phase velocity, namely

$$\dot{\sigma} = (1 - n_b)\,(A_b/A_s)^2 = (1 - n_b) \cos^2\sigma + (1 - n_a) \sin^2\sigma, \tag{6.5}$$

The first expression shows that the energy transport, $\dot{\sigma}A_s^2$, is constant. The second expressions shows that the phase velocity changes continuously with the phase of the wave, having the extreme values in the non-tilting states.

This result is readily understood from the forcing action of each component wave on the other. Consider for example the non-tilting b-state where the component fields are in phase with equal amplitudes (see Fig. 6). The upper field, if operating alone, would propagate the upper deformation upwind *through the air* as a simple neutral Rayleigh wave with the speed $U/\varkappa$. The lower field, acting in the same sense, will augment this propagation. Its intensity is reduced by the factor $\alpha = e^{-\varkappa}$ at the upper boundary and its contribution to the phase velocity of the upper wave is reduced by the same factor. So the upper wave moves intrinsically upwind through the b-state with the speed $U(1 + \alpha)/\varkappa$. Because of the symmetry the lower wave has the same upwind propagation through the air. The air moves downwind with the speed U at both boundaries in the symmetric frame, so in this frame both waves move *downwind* through the b-state with the speed $U(1 - n_b)$. In the non-tilting a-state the upper and lower fields are opposing each other so, for precisely the same reason, the symmetric wave moves downwind through the a-state with the speed $U(1 - n_a)$.

Since $n_a = (1 - \alpha)/\varkappa < 1$ for all wave lengths, all waves move downwind through the a-state. As soon as the wave leaves the a-state the lower field begins to augment the amplitude of the upper deformation and vice versa. The wave starts growing when it leaves the a-state. However, the wave of $n_b = 1$, which has the wave number

$$\varkappa_s = 1 + \alpha_s = 1.2785\ldots, \qquad (L_s = 4.9d) \tag{6.6}$$

has a stationary neutral b-state. Shorter waves move progressively downwind at all times with rhythmic variations of amplitude and speed. They move rapidly with mini-

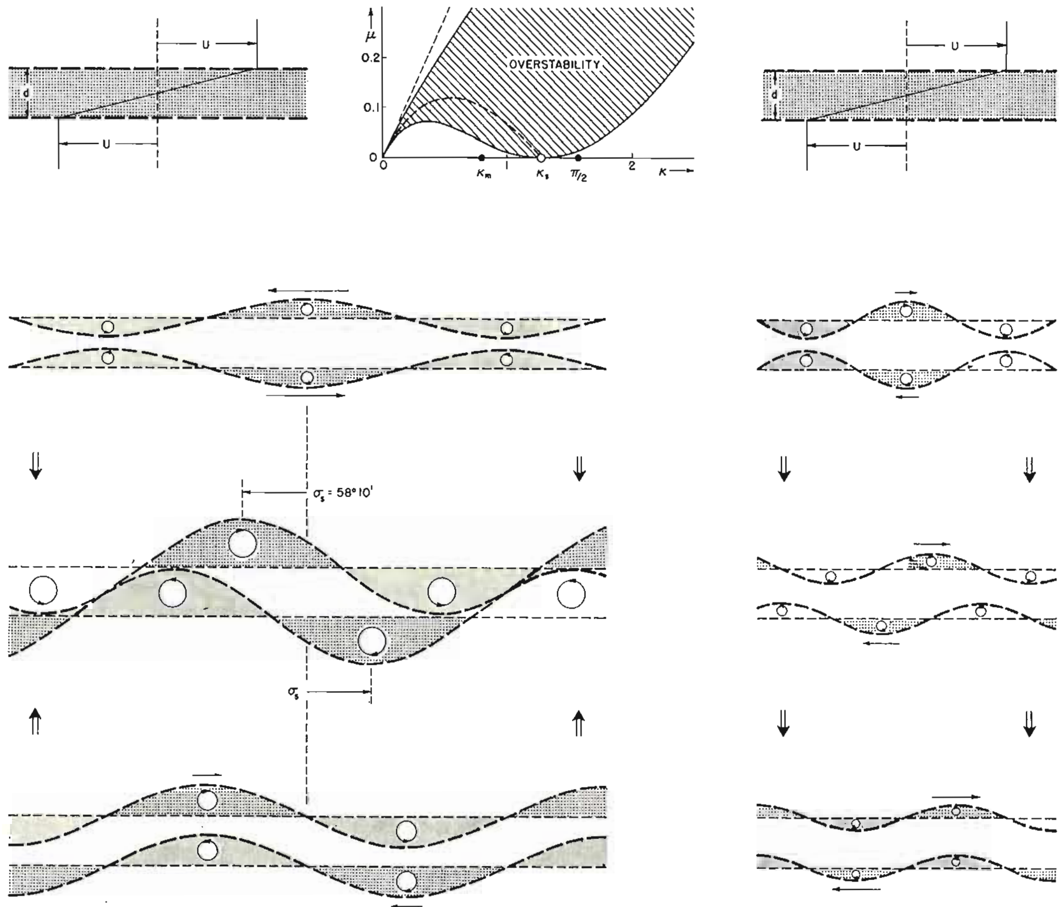

Fig. 6: Evolution of symmetric waves in an isentropic (homogeneous) shear layer.

mum amplitude through the a-state and slowly with maximum amplitude through the b-state (see fig. 6).

The longer ($\varkappa < \varkappa_s$)-waves move downwind through the a-state and upwind through the b-state. From either non-tilting state they approach the same state somewhere in between with a downwind tilt from the a-state. As this state of stationary phase σ_s is approached, the wave slows down and its energy grows in accordance with the law of constant energy transport (6.5).

The state of stationary phase ($\dot{\sigma} = 0$) of the wave, as obtained from (6.5), is

$$\tan^2\sigma_s = -\frac{1 - n_b}{1 - n_a} = \frac{a + (1 - \varkappa)}{a - (1 - \varkappa)}. \tag{6.7}$$

The position of stationary phase is determined by the ratio of the phase speeds in the non-tilting states. A wave just a little longer than the critical $\varkappa_s$-wave moves very slowly upwind through the b-state and rapidly downwind though the a-state. It comes to rest just a little upwind from the b-state. The ($\varkappa = 1$)-wave moves with the same speed in opposite directions through the non-tilting states and comes to rest half way between them, 45° downwind from the a-state. A wave very much longer than the thickness of the shear layer moves very fast upwind through the b-state and very slowly downwind through the a-state. To the first order of $\varkappa$ the stationary phase is $^1/_2\varkappa$ downwind from the a-state, so the downwind displacement of the upper crest from the lower crest is equal to the thickness of the shear layer.

In the state of stationary phase the wave keeps on growing at a rate which is proportional to the instantaneous strength of the field, so the wave has here a constant growth rate,

$$\frac{d}{dt}(\ln A_s) = n. \qquad \text{(when } \sigma = \sigma_s\text{)}.$$

This growth rate depends upon the phase and hence is a function of the wave length. The evolution of the wave in its approach toward the state of stationary phase from an initial b-state is represented analytically by the equations in (6.3). For the long ($n_b > 1$)-waves the parameter n_R^2 in (6.2) is negative, so the trigonometric functions of $n_R t$ in (6.3) are here the corresponding hyperbolic functions of nt where

$$n^2 = (1 - n_a)(n_b - 1) = [\alpha^2 - (1 - \varkappa)^2]/\varkappa^2 = -n_R^2,$$

and n is the asymptotic growth rate in the state of stationary phase ($\sigma \to 0$). In arbitrary units with the frequency unit Uk restored the growth rate is given by

$$\text{(6.8)} \qquad \left(\frac{\varkappa n}{kU}\right)^2 = \left(\frac{nd}{U}\right)^2 = \alpha^2 - (1 - \varkappa)^2.$$

It is zero for the $\varkappa_s$-wave, and it approaches zero again for waves very much longer than the depth of the shear layer. For the very long waves the growth rate has ultimately the value Uk, which is the growth rate for all waves in a vortex sheet: For waves much longer than the depth of the shear layer, the shear layer behaves dynamically as a vortex sheet. The wave of maximum growth rate has the wave number for which $dn/d\varkappa = 0$. From (6.8) that wave number is

$$n(\max): \varkappa_m = 1 - \alpha_m^2 = 0.8 \qquad (L_m = 7.9d).$$

This wave of maximum growth rate is shown in fig. 6. It is about eight times longer than the depth of the shear layer. From (6.8) its growth rate is

$$\text{(6.9)} \qquad n(\max) = 0.4U/d = {}^1/_2 Uk_m \qquad (L_m = 7.9d).$$

It is precisely one half the growth rate of the same wave if the depth of the shear layer shrinks to zero.

The stationary phase of the wave of maximum growth rate, $\varkappa_m = 0.8$, is from (6.7) $\sigma_m = -58°10'$. It is about 32° downwind from the a-state. Fig. 6 shows the evolution of this wave from an inital a-state or b-state. As the wave moves out of the a-state the rotational shear layer becomes periodically inflated and deflated, with the inflated parts centered downwind from the crests of the upper boundary. As the evolution continues, it is evident that the kinematics of the wave places an upper *kinematic* limit on the linear evolution, namely the moment when the deflated parts of the shear layer have no thickness in the middle. If the wave of maximum growth rate is started from an a-state which is one per cent of the wave length ($A_a = 0.01\ L_m$) and the linear evolution is extrapolated to the kinematic limit, the wave will have reached very nearly to the state of stationary phase at that time, so the limiting interface amplitude A_m is given by $2A_m \cos \sigma_m = d$, so we have

$$A_m k_m = {}^1/_2 \varkappa_m \sec \sigma_m = 0.75. \qquad \text{(kinematic limit)}$$

This value does not satisfy the condition for the linear approximation ($A_s k \ll 1$), so here the evolution of the wave is certainly no longer linear. The non-linear terms in the dynamic equations which have been ignored become increasingly important as the amplitude grows, and what ultimately happens to the wave can not be predicted by linear theory. However it is plausible that the periodic inflation and deflation of the shear layer which develops during the linear evolution will tend toward separation of the rotating air in the shear layer into elongated regions which tilt upwind from the shear of the initial basic flow. These regions of rotating air will probably retain their identity for some time and keep on rotating about their centers of mass, each behaving roughly as KIRCHHOFF's isolated elliptic vortex [5].

7. The shear layer with static stability across the central level. Let us now examine the symmetric wave (4.1) in this more general system. The central temperature interface conditions (4.3) for this wave are

$$\dot{A} = n_s^2 \varkappa A_T, \qquad \varkappa \dot{A}_T = -(A + 2\sqrt{a}\xi), \tag{7.1}$$

or with A_T eliminated

$$\ddot{A} = -n_s^2 (A + 2\sqrt{a}\xi). \tag{7.2}$$

The sum of the kinematic conditions (4.4) at the boundaries of the shear layer gives

$$\sqrt{a}\, A/\varkappa = (1 - n_b)\xi - \dot{\eta},$$

where n_b is the frequency parameter in (6.1). Elimination of A from this equation and (7.2) gives

$$(1 - n_b)\ddot{\xi} - \dddot{\eta} = -n_s^2 [(1 - n_a)\xi - \dot{\eta}].$$

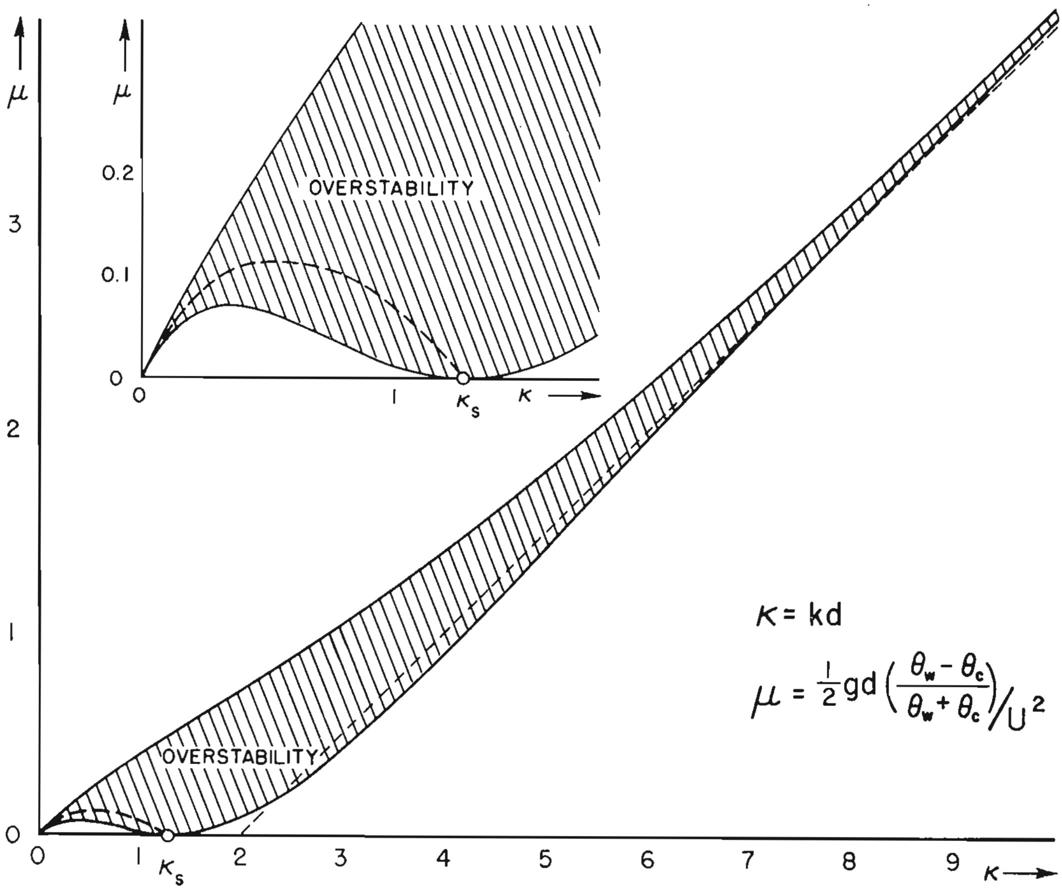

Fig. 7: Stability diagram for a shear layer with static stability across the center level.

This equation in combination with the difference between the kinematic conditions in (4.4), namely

$$(1 - n_b)\ddot{\xi} + n_s^2(1 - n_a)\xi = \dddot{\eta} + n_s^2\dot{\eta}, \tag{7.3}$$

$$(1 - n_a)\eta = -\dot{\xi},$$

describe implicitly the evolution of the symmetric vorticity wave (4.1) from an arbitrary tilting state. We recall that in the absence of static stability at the central level the long ($n_b > 1$) waves have two states of stationary phase. Let us examine whether the wave in (7.3) has a state of stationary phase, $\sigma = \sigma_s$. In such a state only the wave amplitude A_s changes and the evolution equations (7.3) reduce to

$$(1 - n_b)\ddot{A}_s + n_s^2(1 - n_a)A_s = (\dddot{A}_s + n_s^2\dot{A}_s) \tan \sigma_s,$$

$$(1 - n_a)A_s = -\dot{A}_s \cot \sigma_s.$$

This system of equations has solutions of the form $A_s \sim e^{nt}$, where n is a root of the system

$$(1 - n_b)n^2 + (1 - n_a)n_s^2 = (n^3 + nn_s^2)\tan\sigma_s, \qquad (7.4)$$
$$(1 - n_a) = - n \cot \sigma_s.$$

Elimination of σ_s and introduction of the two parameters

$$n_R^2 \equiv (1 - n_a)(1 - n_b), \qquad [n_{a/b} \equiv (1 \pm a)/\varkappa] \qquad (7.5)$$
$$m^2 \equiv {}^1/_2(1 - n_a)n_s, \qquad [n_s^2 \equiv 2\mu/\varkappa]$$

gives a bi-quadratic equation for n, namely

$$n^4 + (n_s^2 + n_R^2)n^2 + 4m^4 = 0. \qquad (7.6)$$

This equation has a double root n^2 when its descriminant is zero, that is, when

$$d \equiv (n_s^2 + n_R^2)^2 - 16m^4 = 0, \qquad (7.7)$$

or

$$n_s^2 \pm 4m^2 + n_R^2 = 0.$$

This condition may be represented graphically by a curve in a $\varkappa,\mu$-diagram (see fig. 7) having the two branches

$$n_s = (1 - n_a) \left| 1 \pm \left(\frac{n_b - n_a}{1 - n_a}\right)^{1/2} \right|. \qquad |n^2| = 2m^2 \qquad (7.8)$$

Both branches have a common tangent, $\mu = {}^1/_2\,\varkappa$, at the origin and the common asymptote $\mu = {}^1/_2\,\varkappa - 1$. The lower branch is tangent to the $\varkappa$-axis at the point of $n_b = 1$, that is at $(\varkappa = \varkappa_s,\ \mu = 0)$.

On the long wave part $(\varkappa < \varkappa_s)$ of the lower branch $n_s^2 + n_R^2 < 0$, so here the double root n^2 in (7.8) is positive. The wave has here two states of stationary phase, one growing and one decaying at the rate $\sqrt{2}m$. On the upper branch and the short wave part of the lower branch the double root is negative. The wave is here a stable wave with the frequency $\sqrt{2}m$. In the region between the two branches the roots of the bi-quadratic equation in (7.6) are complex. The waves have here no state of stationary phase. We shall examine these waves in section 9 below. It turns out that they perform exponentially growing oscillations. EDDINGTON has named this type of motion *overstability*. The name is unfortunate, but it has been introduced into hydrodynamical literature by CHANDRASEKHAR [6] and other authors. Before we consider the waves in this "overstable" region bounded by the two curve branches in (7.8), let us examine the critical waves on the lower $(\varkappa < \varkappa_s)$-boundary for which the frequency equation (7.6) has a positive double root of n^2, and hence the waves have two states of stationary phase.

8. The critical ($\varkappa < \varkappa_s$)-waves on the lower boundary of the overstable region. In the states of stationary phase the growth rate n is from (7.5—8) given by

$$n^2 = 2m^2 = n_s(1 - n_a) = (1 - n_a)^2 \left[\left(\frac{n_b - n_a}{1 - n_a}\right)^{1/2} - 1\right]. \tag{8.1}$$

The growing state is tilting upwind from the b-state (see 7.4) and the decaying state is tilting symmetrically downwind. The stationary phase σ_s is given by

$$\tan^2 \sigma_s = \left(\frac{n}{1 - n_a}\right)^2 = \left(\frac{n_b - n_a}{1 - n_a}\right)^{1/2} - 1 = \frac{n_s}{1 - n_a}. \tag{8.2}$$

Near the short wave end of this spectral band ($\varkappa \to \varkappa_s$) where $n_b \to 1$ the wave is very nearly the stationary neutral Rayleigh wave in the barotropic shear layer ($n \to \sigma_s \to 0$). For waves very much longer than the depth of the shear layer the ($\varkappa \ll 1$)-wave is very nearly the stationary neutral Helmholtz wave in the sliding boundary between isentropic layers of different densities ($n \to 0$, $\sigma_s \to 90°$).

The wave whose stationary phase is 45° has also a simple structure (see the center wave diagram in fig. 8). Its wave number and growth rate are

$$\begin{aligned} \varkappa &= 1 - \tfrac{1}{2}a = 0.768 \\ \pm n = n_s &= 1 - n_a = \tfrac{1}{2}a/\varkappa = \varkappa^{-1} - 1 = 0.3 \qquad (\mp\sigma_s = 45°). \end{aligned} \tag{8.3}$$

It is just a little longer than the wave of maximum growth rate in the barotropic shear layer (6.9), and its growth rate is 43 per cent less.

It is not difficult to predict the relative strength of the dynamic vorticity field along the central interface in this wave. It must be just strong enough to cancel the propagation which the waves at the boundaries of the shear layer would have in its absence. Since these waves are 90° out of phase, each would be propagated only by its own field with the intrinsic phase velocity $\varkappa^{-1}$, that is with the upwind speed $\varkappa^{-1} - 1$ in the symmetric frame. To cancel this propagation the dynamic vorticities at the central level must have an amplitude A such that

$$\sqrt{\tfrac{1}{2}a}\, A\varkappa^{-1} + (\varkappa^{-1} - 1)A_s = 0, \text{ or } -A/A_s = \sqrt{\tfrac{1}{2}a}.$$

This result comes of course also from the general evolution equation (7.2) with the parameters in (8.3) substituted.

In the same way the amplitude of the central interface may be predicted from the fact that its growth rate must be equal to that of the shear layer boundaries. The latter is readily seen to be

$$\frac{\dot{A}_s}{A_s} = \frac{aA_s/\varkappa + \sqrt{\tfrac{1}{2}a}\, A/\varkappa}{A_s} = \tfrac{1}{2}a/\varkappa.$$

The same growth rate for the central temperature interface amplitude gives

$$\frac{\dot{A}_T}{A_T} = \tfrac{1}{2}a/\varkappa = \frac{A/\varkappa + \sqrt{2a}\,A_s/\varkappa}{A_T} = \frac{A/\varkappa}{A_T}\,.$$

This result agrees with the evolution equation for A in (7.1), which for the wave in (8.3) gives $A/A_T = \varkappa n_s = {}^1/_2 a$.

The stationary growing wave in (8.3) accordingly has the amplitude ratios

$$A/A_s = A_s/A_T = -\sqrt{\tfrac{1}{2}a} = -0.48. \qquad (\sigma_s = -45^\circ). \tag{8.4}$$

The central dynamic vorticity is about one half of the kinematic vorticity at the boundaries of the shear layer, and the amplitude of these boundaries is about one half of the central interface amplitude.

The dynamic growth mechanism of the wave is quite clear: In the absence of the dynamic vorticities the field from the kinematic vorticities would augment the amplitudes of all three boundaries and propagate the upper and lower wave symmetrically upwind. The field from the dynamic vorticities at the central interface cancels the propagation of the outer waves and reduces the growth of the amplitudes. The overweight of the deformed central interface in turn augments the central dynamic vorticity field. With the amplitude ratios in (8.4) the fields are properly "tuned" to keep on growing at equal rates.

In the corresponding isentropic shear layer the wave in (8.3) would have the stationary phase $\sigma_s = -60^\circ$ (see 6.7) and the growth rate in (8.3) would be augmented by the factor $\sqrt{3}$.

The two states of stationary phase in (8.3) are a pair of normal modes of the shear layer. The resultant of these modes with equal or opposite initial amplitudes is a symmetric wave which initially has a non-tilting state. The non-tilting b-state of the wave is shown in the upper wave diagram in fig. 8. With the initial b-state amplitude of the shear layer boundaries chosen as amplitude unit, the component normal modes have the upper interface evolutions

$$\begin{aligned} z_1^+ &= \tfrac{1}{2}\sqrt{2}\, e^{nt} \cos(x + 45^\circ), \\ z_1^- &= \tfrac{1}{2}\sqrt{2}\, e^{-nt} \cos(x - 45^\circ), \end{aligned} \tag{8.5}$$

and the resultant wave at the upper interface is

$$z_1 = \mathrm{ch}\, nt \cos x - \mathrm{sh}\, nt \sin x = A_s \cos(x - \sigma).$$

The phase of the wave is given by $\tan\sigma = -\mathrm{th}\, nt$. The wave leaves the b-state with the upwind speed $n = 1 - n_a$ and moves with decreasing speed towards the asymptotic state of stationary phase $\sigma_s = -45^\circ$. Again the initial b-state amplitude of the central dynamic vorticity field may be predicted from the phase velocity at the shear layer boundaries. Its function is to reduce this phase velocity from the isentropic layer value $n_b - 1$ to the value $1 - n_a$, so we have

$$-\sqrt{a}A\varkappa^{-1} = (n_a + n_b - 2)A_s = 2(1 - \varkappa)A_s\varkappa^{-1}$$

which from (8.3) gives $A = -\sqrt{a}A_s$. Equation (7.2) gives precisely this value for the b-state ($\sigma = 0$), and for an arbitrary later state

$$A = -\sqrt{a}\xi = -\sqrt{a}\,\mathrm{ch}\,nt.$$

In the initial b-state the dynamic vorticity field is neutral, so the central interface has no initial deformation, but it is being deformed at the initial rate $\dot{A}_T = -\sqrt{a}/\varkappa$.

The resultant of the normal modes in (8.5) with opposite initial amplitudes has the upper interface evolution

$$z_1 = \mathrm{sh}\,nt\cos x - \mathrm{ch}\,nt\sin x = A_s\cos(x - \sigma). \tag{8.6}$$

This wave moves downwind from the initial a-state shown in the lower wave diagram in fig. 8 with the initial phase velocity $1 - n_a$. This a-state is neutral, so the dynamic sliding vorticity is absent ($A = -\sqrt{a}\xi$), but it is growing at the rate

$$\dot{A} = -\sqrt{a}\,n\,\mathrm{ch}\,nt = n_s^2\varkappa A_T, \text{ so } A_T = -(2/\sqrt{a})\,\mathrm{ch}\,nt.$$

The initial a-state has the amplitude ratio $A_{Ta}/A_{sa} = 2/\sqrt{a} = 2.8$. The central interface deformation is about three times larger than the deformations of the shear layer boundary. This is a rather artificial initial disturbance. A more natural initial state would be one with the central interface having the same deformation as the outer boundaries and no sliding vorticities.

This "equal deformation" a-state may be represented as the resultant of two a-states, namely: (i) the a-state of the wave in (8.6), and (ii) another a-state whose amplitude is augmented by the factor $(2/\sqrt{a} - 1)$ and having no deformation and vorticity at the central interface. The evolution of this second component is obtained from the second pair of normal modes whose amplitudes are proportional to $t\exp(\pm nt)$. Choosing for the moment its a-state amplitude as unit, its wave elements are readily found from (7.1—3) to be

$$\begin{aligned} \xi &= nt\,\mathrm{ch}\,nt, & A &= \sqrt{a}\,(\mathrm{sh}\,nt - nt\,\mathrm{ch}\,nt), \\ -\eta &= nt\,\mathrm{sh}\,nt + \mathrm{ch}\,nt, & -A &= (2/\sqrt{a})\,nt\,\mathrm{sh}\,nt. \end{aligned} \tag{8.7}$$

Also this wave leaves the a-state with the downwind speed $1 - n_a$ and has the asymptotic stationary phase $\sigma_s = -45°$. Putting now the two waves in (8.6) and (8.7) together, the latter augmented by the factor $2/\sqrt{a} - 1 = 1.8$, the resultant wave has the evolution

$$\begin{aligned} \xi &= \mathrm{sh}\,nt + 1.8\,nt\,\mathrm{ch}\,nt, & A &= \sqrt{a}\,(0.8\,\mathrm{sh}\,nt - 1.8\,nt\,\mathrm{ch}\,nt), \\ -\eta &= 2{,}8\,\mathrm{ch}\,nt + 1.8\,nt\,\mathrm{sh}\,nt, & -A_T &= 2.8\,(\mathrm{ch}\,nt + 1.8\,nt\,\mathrm{sh}\,nt). \end{aligned}$$

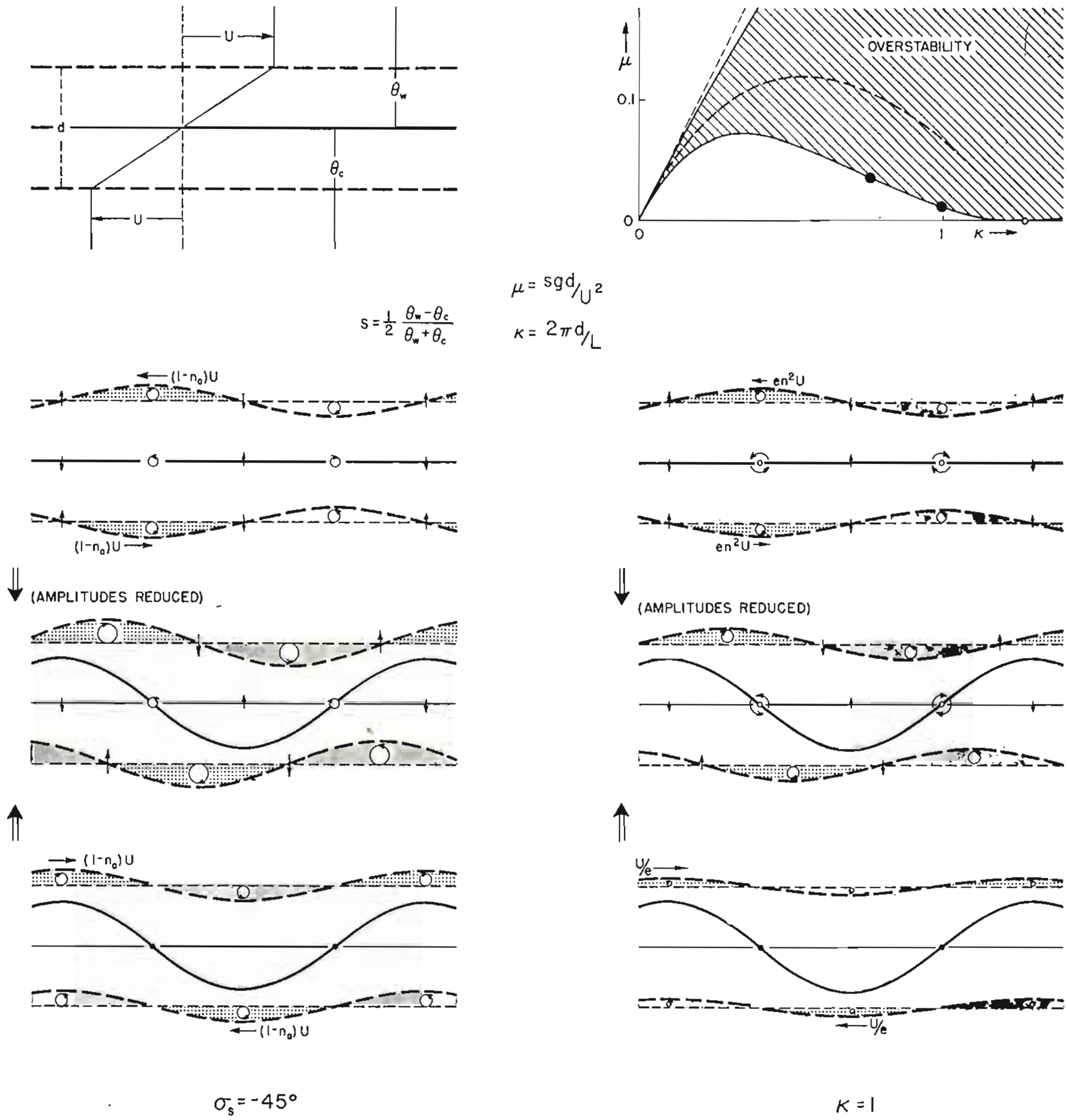

Fig. 8: Evolution of the waves at the transition between instability and overstability.

This wave starts from an initial "equal deformation" a-state ($A_{sa} = A_{Ta}$) and approaches the state of stationary phase $\sigma_s = -45°$. Ultimately the evolution is dominated by the component in (8.7) and the amplitude ratio has the asymptotic value $A_s/A_T = \sqrt{\tfrac{1}{2}\alpha} = 0.48$. The *kinematic* limit of the linear evolution of this wave comes when the central interface touches the boundaries of the shear layer, that is when its amplitude has reached the value $A_T = 0.65d = 0.08L$.

Let us compare the wave just examined with the $(\varkappa = 1)$-wave on the lower boundary of the overstable region (see fig. 8). The dynamics of the $(\varkappa = 1)$-wave is also rather simple: the waves at the boundaries of the shear layer are propagated upwind through the air by their own fields with the intrinsic phase velocity $\varkappa^{-1} = 1$, and hence would remain stationary in the symmetric frame if the other fields were absent. From (8.1) and (8.2) the growth rate and stationary phase of the $(\varkappa = 1)$-wave are given by

$$(en)^2 = en_s = \tan^2\sigma_s = \sqrt{2} - 1. \qquad (\sigma_s = 32°46') \tag{8.8}$$

In the state of stationary phase the contributions to the propagation of the outer waves from the two other fields must cancel:

$$aA_s \cos 2\sigma_s + \sqrt{a}\, A \cos \sigma_s = 0,$$

so the growing mode has the amplitude ratio

$$- A/A_s = \sqrt{a} \cos \sigma_s\, (2 - \sec^2 \sigma_s) = \cos \sigma_s\, (2 - \sqrt{2})/\sqrt{e} = 0.3.$$

The equal growth rates of the deformations namely,

$$\frac{aA_s \sin 2\,\sigma_s + \sqrt{a}\, A \sin \sigma_s}{A_s} = - \frac{2\sqrt{a}A_s \cos \sigma_s + A}{A_T},$$

give the second amplitude ratio of the growing mode, $- A_s/ A_T = \sin \sigma_s/\sqrt{e} = 0.33$. The general evolution equations in (4.1) give of course the same values. The central interface deformation is about three times the deformation of the shear layer boundaries.

An initial non-tilting b-state of this wave as obtained from the pair of normal modes in (8.8) have the wave elements

$$\xi = A_s \cos \sigma = \cos \sigma_s \operatorname{ch} nt, \qquad A = - n_s\xi\sqrt{2e},$$

$$\eta = A_s \sin \sigma = \sin \sigma_s \operatorname{sh} nt, \qquad A_T = - n_s^{-1}\eta\sqrt{2/e}.$$

The wave leaves the b-state with the upwind phase velocity $en^2 = 0.15$ and the amplitude ratio $- A/A_s = 0.355$. In the same way we find that the corresponding symmetric wave leaves the a-state with the downwind phase velocity $1 - n_a = e^{-1}$, and the amplitude ratio $A_{Ta}/A_{sa} = 5.6$. The evolution from an equal deformation a-state of the $(\varkappa = 1)$-wave would be represented as the resultant of this symmetric wave and another constructed from the $(t \exp nt)$-modes whose amplitude is 4.6 times as large. Ultimately this latter component would dominate as the wave approaches the stationary phase in (8.8) with the asymptotic amplitude ratio $A_T/A_s = 3$.

The two waves shown in fig. 8 have remarkably similar growth rates, namely

(8.3) $\varkappa = 0.768$: $n = 0.232(U/d)$, $- \sigma_s = 45°$.

(8.8) $\varkappa = 1$: $n = 0.236(U/d)$, $- \sigma_s = 32°46'$.

The longer wave has the more favorable tilt for efficient growth ($\sigma_s = 45°$) but its static stability at the central interface is more than twice that of the ($\varkappa = 1$)-wave. The wave of maximum growth rate on this overstability boundary is about half way between the two waves in fig. 8. Its wave number and growth rate are $\varkappa = 0.906$ and $n = 0.243(U/d)$. It is interesting to note that the rather weak static stability at the central interface of these waves ($\mu \sim 0.02$) reduces their growth rate to about 60 per cent of the isentropic shear layer value.

9. Waves in the overstable region. In this part of the $\mu,\varkappa$-diagram the discriminant of the frequency equation (7.6) is negative, so the waves have complex frequencies. This means that the central interface performs standing oscillations with exponentially growing amplitude. Let us consider the waves for which the coefficient of the linear term in the frequency equation is zero, that is

$$n_s^2 = -n_R^2 = (n_b - 1)(1 - n_a). \tag{9.1}$$

These are the waves for which the growth rate of the simple Rayleigh wave in the homogeneous shear layer is equal to the frequency of the simple gravity wave in the central temperature interface. The condition (9.1) is represented by a curve in the $\varkappa,\mu$-diagram (see fig. 7) which leaves the origin with the tangent slope $\mu = {}^1/_2\varkappa$ and returns to the $\varkappa$-axis at the point $\varkappa = \varkappa_s$ along the tangent $\mu = (\varkappa_s - 1)(\varkappa_s - \varkappa)$. On this curve the frequency equation (7.6) has the complex roots

$$n = \pm (1 \pm i)m, \tag{9.2}$$

so the waves have no state of stationary phase. However it is readily seen that the general evolution equations (7.3) have here solutions of the form

$$\xi,\eta \sim \exp [\pm (1 \pm i)mt].$$

By a linear combination of these we construct the real solution

$$\xi = \sqrt{2}\, e^{mt} \cos (mt + {}^1/_4\, \pi), \tag{9.3}$$

$$\eta = n_s\, e^{mt} \sin mt/m.$$

This wave has initially the non-tilting b-state shown in the upper left wave diagram in fig. 9 for the wave of $\varkappa = 1$. Its phase has the evolution

$$\tan \sigma = \frac{n_s}{m} \frac{\sin mt}{\cos mt - \sin mt}. \tag{9.4}$$

It moves progressively downwind at all times. Its phase velocity is given by

$$\frac{1}{\dot{\sigma}} = \frac{1 - \sin 2mt}{n_s} + \frac{1 - \cos 2mt}{1 - n_a}. \tag{9.5}$$

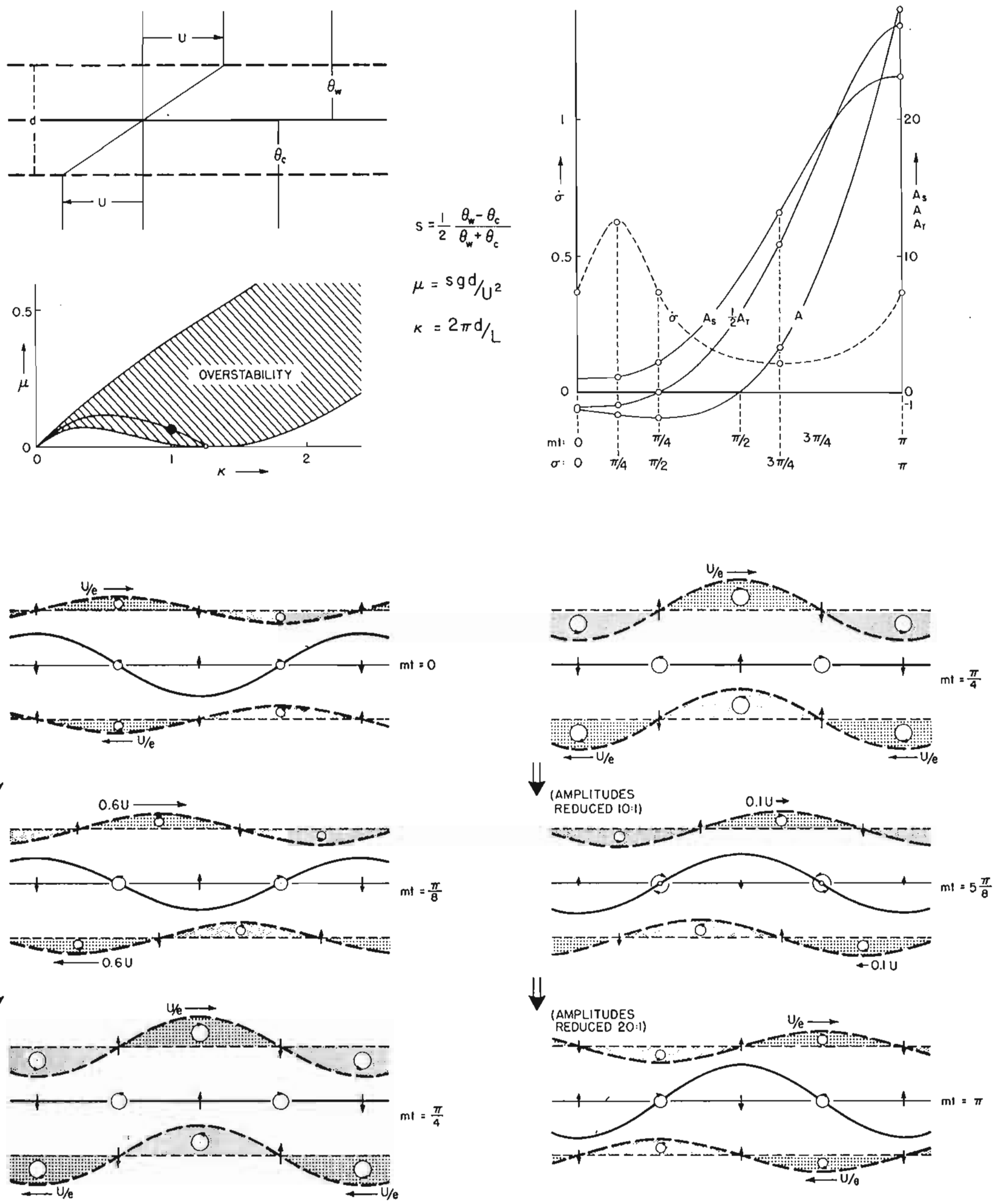

Fig. 9: Evolution of an overstable wave.

The wave moves through the b-state ($mt = \sigma = 0$) with the speed n_s and it moves through the a-state ($2mt = \sigma = 90°$) with the speed $1 - n_a$. However these are not the extreme values of the phase speed as was the case when the wave has a state of stationary phase. The wave in (9.3) has the extreme phase speeds $\dot{\sigma}_m$ at the times when

$$(9.6) \qquad 2mt = \tau = \tan^{-1}\left(\frac{1 - n_a}{n_s}\right). \qquad (\ddot{\sigma} = 0)$$

These extreme values are given by

$$(9.7) \qquad \frac{1}{\dot{\sigma}_m} = \frac{1}{n_s} + \frac{1 - \sec\tau}{1 - n_a}.$$

From (7.1) the evolutions of the wave elements at the central level are

$$(9.8) \qquad \begin{aligned} A &= - 2\sqrt{2a}\cos\tau\, e^{mt}\cos(mt - \tau + {}^1/_4\pi) \\ \varkappa A_T &= + 2\sqrt{a}\sin\tau\, e^{mt}\sin(mt - \tau)/m. \end{aligned}$$

It may be noted that the non-dimensional time of extreme wave speed is the complement of the stationary phase of the same wave in the isentropic shear layer (see 6.7)

$$\cot^2\tau = \left(\frac{n_s}{1 - n_a}\right)^2 = \frac{n_b - 1}{1 - n_a} = \frac{a - (\varkappa - 1)}{a + (\varkappa - 1)}$$

Waves very much longer than the depth of the shear layer ($\varkappa \ll 1$) reach their maximum speed a short time after leaving the b-state. The short waves ($\varkappa \to \varkappa_s$) have maximum speed a short time before they reach the a-state. The wave mechanism is rather clearly exhibited by the ($\varkappa = 1$)-wave which has the extreme speeds half way between the non-tilting states, when the upper and lower waves are 90° out of phase.

The evolution of the ($\varkappa = 1$)-wave is shown in fig. 9. Its basic parameters have the values

$$n_s = 1 - n_a = a = \sqrt{2}m = e^{-1},\ \tau = {}^1/_4\pi. \qquad (\varkappa = 1)$$

The phase of the wave is therefore

$$\tan\sigma = \sin mt/\cos(mt + {}^1/_4\pi), \qquad (\varkappa = 1).$$

and the phase velocity is given by

$$e\dot{\sigma} = [2 - \sqrt{2}\cos(2mt - {}^1/_4\pi)]^{-1}.$$

The three wave amplitudes have the evolutions

$$\begin{aligned} A_s^2 &= \exp(2mt - 1)/\dot{\sigma}, \\ A &= - 2\exp(mt - {}^1/_2)\cos mt, \qquad (\varkappa = 1). \\ A_T &= - 2\exp(mt + {}^1/_2)\sin(mt - {}^1/_4\pi). \end{aligned}$$

These evolutions through a half period from an initial b-state through an a-state and on to the next b-state are shown in the upper right diagram in fig. 9. The left column of wave diagrams in the figure illustrates the evolution of the entire wave from the b-state to the a-state. The right column shows the evolution from the a-state to the next b-state. The evolution of the wave may be anticipated in a qualitative way by inspection of these diagrams:

$(mt = 0)$: In the initial b-state the ratio of the vorticity amplitudes is $-A/A_s = 2\sqrt{a} = 1.2$. The central level is therefore a nodal plane of the resultant field so all deformations are instantaneously neutral in the b-state $(\dot{A}_s = \dot{A}_T = 0)$. The sliding vorticity across the central temperature interface on the other hand is being augmented by overweight of this interface. The deformations of the shear layer boundaries are moved by all three component fields. They would remain stationary in the symmetric frame if propagated by their own local fields only. The field from the other boundary would give the wave the upwind speed U/e. The dynamic vorticities in the middle would propagate the wave in the opposite direction with the speed $2U/e$. So the resultant propagation is downwind through the b-state with the speed U/e. As the outer waves leave the b-state their resultant field can no longer neutralize the action of the growing dynamic vorticity field at the central level: The temperature deformation decays and the growth of the dynamic vorticities slows down as the wave leaves the b-state. At the same time the downwind propagation of the outer waves is speeded up and they begin to grow. This is clearly seen by inspection of the wave at the time when it has reached the state of $\sigma = 45°$, which happens at the time

$(mt = \pi/8)$: This state is shown in the left middle wave diagram in fig. 9. At this moment the outer waves are propagated by the central field only. If the vorticity amplitude ratio had remained unchanged the wave speed would have been augmented by the factor $\sqrt{2}$ and the growth rate would have had the instantaneous value $\dot{A}_s/A_s = (\sqrt{2} - 1)\alpha$. However it is evident that the dynamic vorticities must have grown relatively more than the kinematic vorticities. So the wave speed and growth rate are somewhat greater than the above values. From this state of $\sigma = 45°$ the wave therefore moves rapidly on to the a-state shown in the left bottom wave diagram. It arrives here at the time of

$(mt = \pi/4)$: At that moment the central deformation has decayed to zero, so the central dynamic vorticity field has now reached its maximum value. It deforms at that moment all three boundaries with its full strength $(\dot{A}_T = \dot{A}_s\sqrt{a} = A)$. The outer waves move downwind through the a-state as in the homogeneous shear layer with the speed $U(1 - n_a) = U/e$. As the wave leaves the a-state a new temperature deformation grows up quite rapidly. In the beginning the growth is mainly caused by the strong dynamic vorticity field at the central level. Later, as the dynamic vorticity field decays, the task of augmenting the central temperature deformation is taken over by the resultant field from the kinematic vorticities at the outer boundaries. The dynamic vorticities are completely annihilated at the time of

($mt = {}^1/_2\,\pi$) *:* At that moment the outer waves have the phase of $\tan\sigma = -\sqrt{2}$ and they move downwind as simple Rayleigh waves (see 6.5) with the speed $\dot\sigma = e^{-1}\cos 2\sigma = (3e)^{-1}$, that is roughly one sixth of the maximum speed in the earlier state of $\sigma = 45°$. As the wave now moves slowly on downwind, the resultant field from the kinematic vorticities have just the right upwind tilt for effective augmentation of both the central interface and the outer boundary deformations, so the deformations have ample time to grow. The wave reaches its most favorable tilt for rapid growth ($\sigma = 3\pi/4$) and the minimum speed at the time of

($mt = 5\pi/8$) *:* This situation is shown in the middle right wave diagram in fig. 9. By now the strong overweights across the central interface have generated a certain amount of dynamic vorticity in the opposite sense. In the absence of this dynamic vorticity field the waves at the outer boundaries would be stationary in this state (see 6.5). But the weak dynamic vorticities are now moving the waves. As the wave leaves this state the by now rapidly growing dynamic vorticity tends to speed up the downwind propagation of the outer waves, but the strong kinematic vorticities at the outer boundaries gradually find themselves in a position to oppose the propagation, so the waves recover their speed rather slowly. The dynamic vorticities also oppose the growth of the boundary deformations. By the time the waves reach the new b-state (shown in the bottom right diagram) the growths of both the central interface and the outer boundary deformations have stopped, and they are again instantaneously neutral.

We have examined the kinematic structure and the dynamic wave mechanism of this ($\varkappa = 1$)-wave in some detail, because it exhibits rather clearly the characteristic features of overstability. The very long waves of $n_s^2 = -n_R^2$ for example have in principle the same behavior. The basic parameters of these long waves are

$$n_s = 1,\quad 1 - n_a = {}^1/_2\varkappa = \tau, \qquad m = {}^1/_2\sqrt{\varkappa},$$

$$\varkappa \ll 1 \qquad \dot\sigma(\max) = 1 + \varkappa/4, \qquad \text{at} \quad \sigma = {}^1/_2\sqrt{\varkappa},$$

$$\dot\sigma(\min) = \varkappa/4, \qquad \text{at} \quad \sigma = 90° + {}^1/_2\sqrt{\varkappa}.$$

In the b-state ($\sigma = mt = 0$) these waves have the amplitude ratios $-A/A_s = 2$, $-A_T/A_s = \sqrt{\varkappa}$. They move downwind with the air ($\dot\sigma = 1$) through this b-state because the vorticity field at the central level cancels the propagation from the kinematic vorticities at the shear layer boundary. For a short while the wave speeds up a little to the maximum value $1 + \varkappa/4$ at $\sigma = {}^1/_2\sqrt{\varkappa}$. Later the wave slows down. It reaches the a-state after a very long time ($\sigma = 2mt = {}^1/_2\pi$) with the speed ${}^1/_2\varkappa$ and lingers for a long time just a little downwind from the a-state where the wave can grow.

CHAPTER II

SHEAR LAYER WITH STATIC STABILITY ACROSS THE BOUNDARIES (MODEL II)

10. The velocity field in a model with bounded outer layers. To satisfy the kinematic condition of zero vertical motion at the outer rigid walls, the streamfunction of the field which is associated with the vorticity $(u^+ - u^-)$ at the *upper* shear layer boundary has above and below the interface the values

$$\psi^+ = \psi_s \operatorname{sh} k(h - z)/\operatorname{sh} kh, \qquad \psi^- = \psi_s \operatorname{sh} k(H + z)/\operatorname{sh} kH. \qquad (H = h + d) \tag{10.1}$$

Here h denotes the depth of the outer layers and d, as before, the depth of the shear layer. From (3.3) the tangential components of this field at the interface are

$$u^+ = \psi_s k \operatorname{cth} kh, \qquad u^- = -\psi_s k \operatorname{cth} k(h + d).$$

The *kinematic* vorticity field $(u^+ - u^-)_s$ associated with the deformation z_s of the upper boundary accordingly gives rise to a Laplacean field in the surrounding fluid whose streamfunction, as in (3.2), has the boundary level value ψ_s such that

$$(u^+ - u^-)_s = \varkappa\psi_s/(^1/_2 d) = Uz_s/(^1/_2 d). \tag{10.2}$$

Here we have introduced the non-dimensional parameter

$$\varkappa = {}^1/_2 kd[\operatorname{cth} kh + \operatorname{cth} k(h + d)]. \tag{10.3}$$

At the lower boundary of the shear layer the field in (10.1) is reduced to the value $\alpha\psi_s$, where

$$\alpha = \operatorname{sh} kh/\operatorname{sh} k(h + d). \tag{10.4}$$

For waves which are very much shorter than the depth of the outer layers these non-dimensional parameters reduce to the earlier unbounded layer values in Chapter I, namely

$$kh \gg 1: \quad \varkappa = kd, \quad \alpha = e^{-\varkappa}. \tag{10.5}$$

At the other end of the spectrum are the waves which are very much longer than the combined depth of the shear layer and one of the outer layers. These very long waves obey the quasi-static theory with good accuracy. For the long quasi-static waves the non-dimensional parameters above have the values

$$k(h + d) \ll 1: \quad \varkappa = 2R(1 + R)(1 + 2R)^{-1}, \quad \alpha = (1 + 2R)^{-1}. \qquad \left(R = \frac{d}{2h}\right). \tag{10.6}$$

The kinematic vorticities at the lower boundary of the shear layer have the same streamfunction as in (10.2) only with the sign reversed so, precisely as in (3.5), the Laplacean streamfunctions associated with the kinematic vorticities have the boundary level values

$$\psi_s = \pm\, (U/\varkappa) z_s. \tag{10.7}$$

The dynamic sliding vorticities $(u^+ - u^-)_T$ across the boundaries, whose changes are governed by the static overweight across the boundaries, give rise to component Laplacean fields whose streamfunction boundary values ψ_T, as in (10.2), are given by

$$(u^+ - u^-)_T = \varkappa \psi_T / (^1/_2 d).$$

The sliding vorticity change associated with the boundary deformation z_s is

$$\frac{D}{Dt}(u^+ - u^-)_T = 2sg \frac{\partial z_s}{\partial x},$$

and the corresponding changes of the streamfunction at the boundary is therefore

$$\frac{D\psi_T}{Dt} = sgd \frac{\partial}{\partial x}\left(\frac{z_s}{\varkappa}\right), \tag{10.8}$$

precisely as in (3.6).

11. The boundary condition for a symmetric wave. As in Chapter I let z_1 and z_2 denote the deformations of the upper and lower boundary of the shear layer. Let now ψ_1 and ψ_2 denote the streamfunction boundary values of the component fields associated with the upper and lower dynamic sliding vorticities across these boundaries. At some initial time the symmetric wave has the boundary deformations

$$\begin{aligned} z_1 &= A_s \cos (kx + \sigma) = \text{Real part } (Z e^{ikx}), \\ z_2 &= A_s \cos (kx - \sigma) = \text{Real part } (Z^* e^{ikx}), \end{aligned} \tag{11.1}$$

where the asterisk denotes the complex conjugate value. The sliding vorticities across the boundaries are associated with Laplacean component fields whose streamfunctions have the boundary values

$$\begin{aligned} \psi_1 &= (U/\varkappa) A \cos (kx + \theta) = \text{Real part } (\zeta e^{ikx}), \\ -\psi_2 &= (U/\varkappa) A \cos (kx - \theta) = \text{Real part } (\zeta^* e^{ikx}). \end{aligned} \tag{11.2}$$

On the right in (11.1) and (11.2) are introduced the complex wave parameters

$$Z = A_s e^{i\sigma}, \quad \zeta = (U/\varkappa) A e^{i\theta} = \xi + i\eta. \tag{11.3}$$

It will be noted that the phase angles σ and θ are measured positive *upwind* from the non-tilting *a-state* of the wave.

The dynamic symmetry of the shear layer assures continued symmetry of the wave in (11.1,2) at all times, with the amplitudes A, A_s and the phase angles σ, θ functions of time which are determined by the dynamic and kinematic conditions at the boundary of the shear layer. If the upper conditions are satisfied the lower conditions are automatically satisfied in the symmetric wave, so it is sufficient to consider the conditions at the upper boundary. We represent the conditions non-dimensionally by using units of length and time such that $U = k = 1$. The dynamic condition (10.8) at the upper boundary, namely

$$\left(\frac{\partial}{\partial t} + \frac{\partial}{\partial x}\right)\psi_1 = (\mu/\varkappa)\frac{\partial z_1}{\partial x}, \qquad (\mu = sgd/U^2)$$

with the wave elements (11.1,2) substituted, becomes

$$\zeta - i\dot{\zeta} = (\mu/\varkappa)\,Z. \tag{11.4}$$

The kinematic condition at the upper interface, as in (4.4), is

$$\left(\frac{\partial}{\partial t} + \frac{\partial}{\partial x}\right) z_1 = \frac{\partial}{\partial x}\left[\psi_1 + z_1/\varkappa + \alpha(\psi_2 - z_2/\varkappa)\right].$$

For the symmetric wave (11.1,2) this condition becomes

$$Z - i\dot{Z} = \zeta + Z/\varkappa - \alpha(\zeta^* + Z^*/\varkappa). \tag{11.5}$$

The symmetric wave in the statically stable shear layer may be regarded as the combination of two distinct symmetric waves, namely: (i) A dynamic *vorticity wave* (ζ), with sliding vorticities along the boundaries of the shear layer, whose instantaneous evolution (11.4) is governed dynamically by the local vorticity accelerations (overweights) of the interface particles in the deformed boundaries. (ii) A *temperature wave* (Z) associated with the deformed boundaries of the shear layer. Its evolution (11.5) is governed kinematically by the entire velocity field of the symmetric wave.

12. The non-tilting states of the symmetric wave. Let r denote the ratio between the amplitudes of dynamic and kinematic vorticity in an arbitrary state of the wave.

$$r = \frac{A}{A_s} = \frac{\text{dynamic vorticity}}{\text{kinematic vorticity}} \tag{12.1}$$

As in Chapter I any non-tilting state with the upper and lower vorticity fields in opposite phase ($\sigma = \theta = 0$) will be called an a-state of the wave, and the non-tilting states with the fields in phase ($\sigma = \theta = 90°$) will be called b-states. The non-tilting states are instantaneously neutral states. The temperature wave is neutral ($\dot{A}_s = 0$) because the vertical motion is zero on the interface crests and troughs. The vorticity wave is neutral because the maximum sliding vorticity is located at the interface crests and troughs where the interface particles are level and have no overweight.

It is easy to predict the phase velocity of the temperature wave in a non-tilting state. If the dynamic vorticity wave is absent the temperature wave is moved by the kinematic vorticities, so it moves as the Rayleigh wave in the isentropic shear layer (6.5), having the intrinsic upwind phase velocities n_a and n_b in the non-tilting states. The dynamic vorticities contribute to the propagation in precisely the same manner, and the two effects are additive. The intrinsic phase velocities with an arbitrary vorticity amplitude ratio r is therefore

(12.2)
$$\dot{\sigma}_a + 1 = n_a(1 + r), \qquad n_a = (1 - \alpha)/\varkappa.$$
$$\dot{\sigma}_b + 1 = n_b(1 + r). \qquad n_b = (1 + \alpha)/\varkappa.$$

These formulas may be obtained by applying the kinematic condition (11.5) to the non-tilting states of the wave.

The phase velocity of the vorticity wave is obtained from the dynamic condition (11.4). The real and imaginary parts of this equation, using (11.3), are

(12.3)
$$A \cos \theta + \frac{d}{dt} (A \sin \theta) = \mu A_s \cos \sigma,$$
$$A \sin \theta - \frac{d}{dt} (A \cos \theta) = \mu A_s \sin \sigma.$$

Multiply the first of these by sin θ and the second by cos θ and substract them. The result is

(12.4)
$$\dot{A}/A = (\mu/r) \sin (\theta - \sigma).$$

The vorticity wave grows if the sliding vorticity maximum is upwind from the interface crest ($\theta > \sigma$) and it decays when its maximum is downwind from the crest, which could be predicted qualitatively by consideration of the overweight. The vorticity wave is neutral whenever the vorticity wave and temperature wave are in phase ($\theta = \sigma$). To find the phase velocity return to (12.3), multiply the upper equation by cos θ and the lower equation by sin θ and add them, thus

(12.5)
$$1 + \dot{\theta} = (\mu/r) \cos (\theta - \sigma).$$

For a given amplitude ratio r, the vorticity wave has the maximum intrinsic speed when it is in phase with the temperature wave, namely

(12.6)
$$1 + \dot{\theta} = \mu/r. \qquad (\theta = \sigma).$$

It will be noted that the dynamic vorticity wave is stationary in the symmetric frame ($\dot{\theta} = 0$) if it is in phase with the temperature wave and has the amplitude ratio $r = \mu$. If the wave has this amplitude ratio in a non-tilting state, the vorticity wave is stationary and from (12.2) the temperature wave has the instantaneous intrinsic upwind phase velocities

(12.7)
$$1 + \sigma_a = n_a(1 + \mu);\ 1 + \dot{\sigma}_b = n_b(1 + \mu) \qquad (A/A_s = \mu).$$

Here $\dot{\sigma}$ denotes the upwind phase velocity of the temperature wave in the symmetric frame. In general a non-tilting state with a stationary vorticity wave ($r = \mu$) has a non-stationary temperature wave. However the wave for which $\dot{\sigma}_a = 0$ in (12.7) has a stationary neutral a-state. The wave of $\dot{\sigma}_b = 0$ has a stationary neutral b-state. The wave numbers of these stationary non-tilting waves are given by

(12.8) The stationary a-wave: $n_a(1 + \mu) = 1.$

The stationary b-wave: $n_b(1 + \mu) = 1.$ $\left(\frac{A}{A_s} = \mu\right)$

The b-wave is shorter than the a-wave. We shall show presently that the shear layer has a pair of unstable modes for all wave lengths in the spectral interval between the stationary waves in (12.8). This result was derived by Taylor and Goldstein for a shear layer between unbounded outer layers.

13. The evolution equations for the vorticity wave. In order to develop the tools for the examination of the symmetric wave in an arbitrary tilting state we return to the dynamic and kinematic conditions in section 11, namely

(11.4) $$\zeta - i\dot{\zeta} = (\mu/\varkappa)Z \quad \text{(Dyn.cond.)}$$

(11.5) $$Z - i\dot{Z} = \zeta + Z/\varkappa - \alpha\,(\zeta^* + Z^*/\varkappa). \quad \text{(Kin.cond.)}$$

Substitute the value of the temperature wave Z from the dynamic condition into the kinematic contition. The resulting equation,

$$\ddot{\zeta} + \frac{\mu + 1}{\varkappa}\,(\zeta - \alpha\zeta^*) - \zeta = -\,2i\dot{\zeta} + \frac{i}{\varkappa}\,(\dot{\zeta} + \alpha\dot{\zeta}^*),$$

has the real and imaginary parts

(13.1)
$$\ddot{\xi} + [n_a(1 + \mu) - 1]\xi = (2 - n_a)\dot{\eta}, \qquad n_a = (1 - \alpha)/\varkappa$$
$$\ddot{\eta} + [n_b(1 + \mu) - 1]\eta = -\,(2 - n_b)\dot{\xi}. \qquad n_b = (1 + \alpha)/\varkappa$$

where $\zeta = \xi + i\eta$ is the vorticity wave in (11.3).

The equations (13.1) govern the evolution of the dynamic sliding vorticity field in the symmetric wave from an arbitrary tilting state. When the solutions of these equations are known, the corresponding evolution of the temperature wave is obtained from (11.4), which have the real and imaginary parts in (12.3).

Before we consider the general solutions of the simultaneous system (13.1), let us examine whether the vorticity field can have a state of stationary phase such that $\dot{\theta} = 0$ and $\theta = \theta_s$.

14. The states of stationary phase of the vorticity wave (the unstable modes). In a state of stationary phase ($\theta = \theta_s = \text{const}$) only the amplitude of the wave can change with time so the evolution equations (13.1) for such a state are

$$\ddot{A} + [n_a(1+\mu) - 1]A = (2 - n_a)\,\dot{A}\tan\theta_s, \tag{14.1}$$
$$\ddot{A} + [n_b(1+\mu) - 1]A = -\,(2 - n_b)\,\dot{A}\cot\theta_s.$$

These equations are evidently different forms of the same equation. It has solutions of the form $A \sim e^{nt}$, where n is a root of the simultaneous quadratic equations

$$n^2 + n_a(1+\mu) - 1 = n(2 - n_a)\tan\theta_s, \tag{14.2}$$
$$n^2 + n_b(1+\mu) - 1 = -\,n(2 - n_b)\cot\theta_s.$$

Elimination of θ_s gives the bi-quadratic "frequency" equation

$$[n^2 + n_a(1+\mu) - 1][n^2 + n_b(1+\mu) - 1] + n^2(2 - n_a)(2 - n_b) = 0. \tag{14.3}$$

If the wave shall have a state of stationary phase we see from (14.2) that the frequency equation must have a positive root n_1^2. The sum of the roots ($n_1^2 + n_2^2$) is never positive, so the frequency equation has one positive root if the constant term is negative, that is if

$$(n_1 n_2)^2 = [n_a(1+\mu) - 1][n_b(1+\mu) - 1] < 0. \qquad (n_1^2 > 0). \tag{14.4}$$

This condition is satsified in the spectral interval between the stationary neutral a- and b-wave in (12.8). Outside of this spectral interval, both n^2-roots of (14.4) are negative, so the wave has here no state of stationary phase. Both pairs of modes are here stable oscillations. Their wave components move progressively downwind at all times with rhythmic variations of amplitude and speed between the extreme values in the non-tilting states. In the spectral interval of (14.4), on the other hand, the shear layer has *one pair* of unstable normal modes, one growing and one decaying at the rate n, where n is the real positive root of the frequency equation (14.3) in this interval. The corresponding states of stationary phase $\theta = \theta_s$ are obtained from (14.2). We see that the growing and decaying modes have equal symmetric phase shifts upwind and downwind from the non-tilting a-state ($\theta = 0$).

The temperature field (boundary deformations) of the unstable modes is obtained from the dynamic conditions (12.4) and (12.5). Putting here $\dot{\theta} = 0$, $\theta = 0_s$, and $\dot{A}/A = n$, the ratio of these equations give

$$n = \tan(\theta_s - \sigma_s). \tag{14.5}$$

where σ_s denotes the stationary phase of the temperature wave measured positive upwind from the a-state. In the growing mode ($n > 0$) the vorticity maximum is upwind from the interface crest where the overweight of the interface particle augments the vorticity. From (12.5) and (14.5) we see that the vorticity ratio $r = A/A_s$ is constant in the unstable modes, so both fields grow or decay at the same exponential rate.

The spectral interval of unstable normal modes in (14.4) may be written

$$(14.6) \qquad (1 - a) < \frac{\varkappa}{1 + \mu} < (1 + a), \qquad \text{(Instability)}$$

where the lower limit is the stationary a-wave and the upper limit is the stationary b-wave. If the outer layers are unbounded ($h \to \infty$) the parameters $\varkappa$ and a have the values in (10.5) for all wave lengths, namely $\varkappa = kd$, $a = e^{-\varkappa}$. The corresponding instability condition in (14.6) was derived by GOLDSTEIN [2]. The boundaries of the unstable spectral band in the unbounded system — the Goldstein lines — in a $\varkappa,\mu$-diagram is shown in fig. 14. The upper boundary — the *a*-line — starts from the origin with the slope $\mu = {}^1/_2\varkappa$. Near the origin ($\varkappa \ll 1$) the stationary a-waves are approximately given by

$$\mu = sgd/U^2 = {}^1/_2 kd \; ; \text{ or } \; k = 2sg/U^2.$$

This result is exact if the depth of the shear layer shrinks to zero. It is the well known value of the wave number of the stationary Helmholtz wave in a statically stable vortex sheet. Waves which are very much longer than the depth of the shear layer have approximately the same behavior as in a vortex sheet.

The lower boundary of the unstable region in fig. 14 — the *b*-line — starts from the point $\varkappa_s$ (see 6.6) with the slope $\mu = \varkappa$. Both lines approach the same asymptote, $\mu + 1 = \varkappa$.

In the system with bounded outer layers the parameters $\varkappa$ and a have the general values in (10.3,4), and the spectral band of instability (14.6) is here

$$(14.7) \qquad \operatorname{cth} kh + \operatorname{cth} {}^1/_2 kd > (1 + \mu)/({}^1/_2 kd) > \operatorname{cth} kh + \operatorname{th} {}^1/_2 kd.$$

If the thickness of the shear layer shrinks to zero, no wave length satisfies the right hand b-wave limit. The vortex sheet has no stationary b-wave. However, as $kd \to 0$, the left hand stationary a-wave limit may be written

$$\operatorname{cth} kh - 2sg/U^2k = ({}^1/_2 kd)^{-1} - \operatorname{cth} {}^1/_2 kd \to - kd/6 \to 0.$$

This is the condition for the stationary Helmholtz wave in the vortex sheet between bounded layers.

In the isentropic shear layer ($\mu = 0$) no wave satisfies the a-wave limit in (14.7). The isentropic shear layer has no stationary a-wave. The condition for the stationary b-wave is here

$$\text{Stationary b-wave:} \qquad \operatorname{cth} kh = ({}^1/_2 kd)^{-1} - \operatorname{th} ({}^1/_2 kd), \qquad (\mu = 0).$$

This condition is represented graphically in a (kd, kh)-diagram by a line which leaves the origin with the slope $h = {}^1/_2 d$ and has the vertical asymptote $kd = \varkappa_s$ of the stationary Rayleigh wave (see 6.6) in the unbounded system.

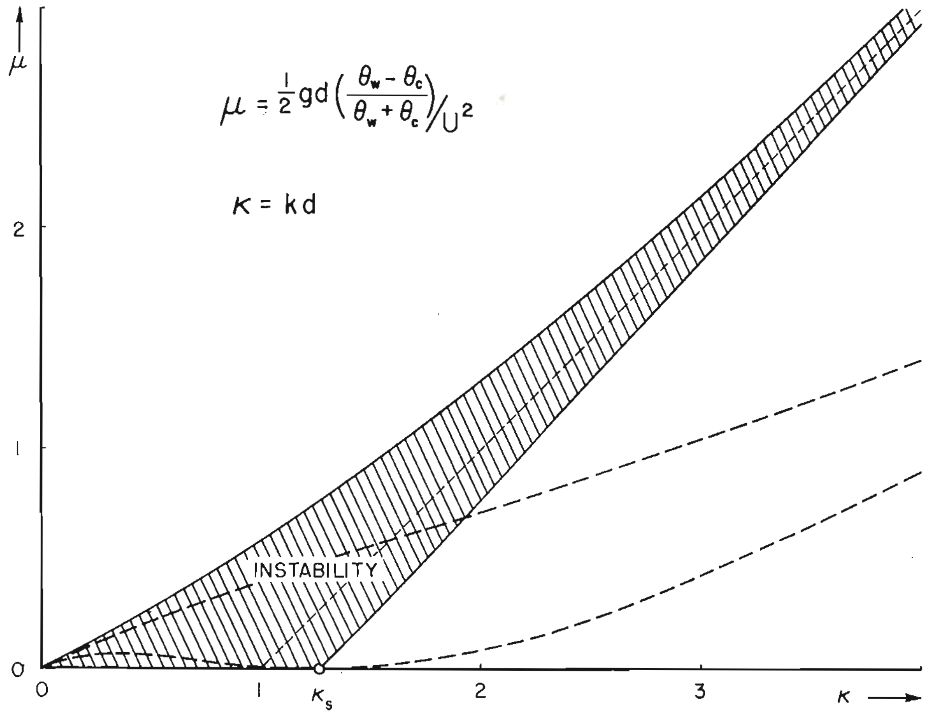

Fig. 14: Stability diagram for a shear layer with static stability across the boundaries.

Waves which are very much longer than the total height of the system, $k(2h + d) \ll 1$, obey the quasi-static approximation with good accuracy. The pressure distribution along the vertical is very nearly hydrostatic in these waves. For the long quasistatic waves the parameters $\varkappa$ and α have the values in (10.6). The corresponding values of the parameters n_a and n_b in (13.1) are

(14.8)
$$n_a = (1 - \alpha)/\varkappa = (R + 1)^{-1}, \qquad k(h + {}^1/_2 d) \ll 1$$
$$n_b = (1 + \alpha)/\varkappa = R^{-1}. \qquad (R = {}^1/_2 d/h).$$

The condition for instability (14.6) for these long quasi-static waves is therefore

(14.9)
$$R > \mu > R - 1. \qquad (R = {}^1/_2 d/h).$$

Let us here replace the "inner" Richardson Number μ whose length parameter is the depth of the shear layer (see 2.3) by the "outer" Richardson Number whose length parameter is the depth of the outer layers, namely

(14.10)
$$\mu_h = \mu/R = 2sgh/U^2.$$

Systems in which this outer Richardson Number has a value in the interval,

(14.11)
$$1 > \mu_h > 1 - 2h/d, \qquad \text{(Quasi-static instability)}$$

have one family of long unstable quasi-static modes. All ($\mu_h > 1$)-systems have quasi-static stability. In the ($\mu_h = 1$)-systems the quasi-static waves have a stationary neutral a-state. In the systems of $d > 2h$ the quasi-static waves have a stationary neutral b-state if $\mu_h = 1 - 2h/d$. These systems have quasi-static instability for values of μ_h in the interval (14.11). They are quasi-statically stable for smaller value of μ_h. Finally the systems of $d < 2h$ have quasi-static instability for all values $\mu_h < 1$. If the depth of the shear layer shrinks to zero, this is the criterion of quasi-static instability in the vortex sheet between bounded layers. It is interesting that this last criterion is independent of the depth of the shear layer as long as it occupies less than one half of the space between the outer boundaries.

15. The evolution of symmetric waves from their non-tilting states. After the preliminary survey of the instability conditions for the shear layer let us now examine the structure of the normal modes. In the unstable spectral interval the vorticity field of the growing mode has the stationary phase θ_s, from (14.2) given by

$$\text{(15.1)} \qquad \tan\theta_s = \frac{n(n_b - 2)}{n^2 + n_b(1 + \mu) - 1} = \frac{n^2 + n_a(1 + \mu) - 1}{n(2 - n_a)}. \qquad (n > 0)$$

Since $n_b(1 + \mu) > 1$ in the unstable region (14.6), the vorticity wave in the growing mode is upwind from the a-state ($\theta_s > 0$) in the long ($n_b > 2$)-waves, and it is downwind from the a-state in the short ($n_b < 2$)-waves. The temperature wave on the other hand is downwind from the a-state ($\sigma_s < 0$) in all growing modes. This is quite obvious for the short ($n_b < 2$)-modes since the temperature wave is downwind from the vorticity wave in all growing modes. For the long ($n_b > 2$)-modes we have from (15.1)

$$0 < \frac{\tan\theta_s}{n} < \frac{n_b - 2}{n_b - 1} < 1,$$

and therefore from (14.5)

$$\tan\sigma_s(1 + n\tan\theta_s) = \tan\theta_s - n < 0, \text{ or } \sigma_s < 0.$$

Let us next examine the evolution of the unstable wave from a non-tilting a-state toward the state of stationary phase of the growing mode. This evolution is obtained as the resultant of the growing and decaying mode with equal initial amplitudes. With the amplitude factor left out the upper vorticity fields of these are

$$\psi_1^+ = {}^1\!/_2 e^{nt}\cos(kx + \theta_s),$$
$$\psi_1^- = {}^1\!/_2 e^{-nt}\cos(kx - \theta_s),$$

and the resultant wave has the upper vorticity field

$$\psi_1 = \text{ch}\, nt\cos\theta_s\cos kx - \text{sh}\, nt\sin\theta_s\sin kx = \frac{A}{\varkappa}\cos(kx + \theta).$$

This wave starts from an initial a-state ($\theta = t = 0$), and its phase has the evolution

$$\tan\theta = \tan\theta_s \,\mathrm{th}\, nt.$$

The phase velocity of the vorticity field in this wave is obtained by time differentiation of this phase equation. Using the value of $\tan\theta_s$ in (15.1), we get

$$\dot{\theta} = \frac{n^2 + n_a(1+\mu) - 1}{2 - n_a}\cos^2\theta + \frac{n^2 + n_b(1+\mu) - 1}{2 - n_b}\sin^2\theta. \tag{15.2}$$

This formula is quite general and applies to the resultant symmetric wave from each of the two pairs of normal modes whose frequency-squares are the two roots, $-n^2$, of the bi-quadratic frequency equation (14.3). In particular the intrinsic upwind phase velocities of the vorticity field in the non-tilting states of these waves are

$$1 + \dot{\theta}_a = \frac{n^2 + \mu n_a + 1}{2 - n_a} = \frac{\mu}{r_a}, \tag{15.3}$$

$$1 + \dot{\theta}_b = \frac{n^2 + \mu n_b + 1}{2 - n_b} = \frac{\mu}{r_b}. \tag{15.4}$$

$$\left(r = \frac{A}{A_s}\right)$$

The corresponding vorticity amplitude ratios r from (12.6) have been added in these formulas. With these amplitude ratios known the intrinsic phase velocities of the temperature wave in the non-tilting states are obtained from (12.2), namely

$$\begin{aligned} 1 + \dot{\sigma}_a &= n_a(1 + r_a), \\ 1 + \dot{\sigma}_b &= n_b(1 + r_b). \end{aligned} \tag{15.5}$$

Finally the symmetric waves from both families of normal modes obey the rules

$$\dot{\theta}_a\dot{\theta}_b = \dot{\sigma}_a\dot{\sigma}_b = -n^2, \tag{15.6}$$

and during their evolution both the vorticity wave and the temperature grow or decay according to the rule

$$A^2\dot{\theta} = \text{const}; \quad A_s^2\dot{\sigma} = \text{const}. \tag{15.7}$$

Let us now examine this evolution in more detail. Inspection of the frequency equation in (14.3) shows that its roots n^2 have simple values for the waves of $n_b = 2$. We shall therefore first consider these waves.

16. The evolution of the symmetric ($n_b = 2$)-waves. The wave numbers of these waves are given by $1 + \alpha = 2\varkappa$, or with these parameters substituted from (10.3,4)

$$\mathrm{cth}\, kh = (kd)^{-1} - \mathrm{th}\, {}^1/_2 kd. \qquad (n_b = 2). \tag{16.1}$$

In a (kd, kh)-diagram this line starts from the origin with the slope $d = h$ and has the vertical asymptote

$$kd = {}^1/_2(1 + e^{-kd}) = 0.74. \qquad (kh \to \infty).$$

So every system with the outer layers deeper than the central layer has one and only one wave number for which $n_b = 2$.

The roots of the frequency equation (14.3) for this wave number are

$$(16.2)\qquad \begin{array}{llll} \text{(i):} & n^2 = -(2\mu + 1), & & n_b = 2, \\ \text{(ii):} & n^2 = 1 - n_a(1 + \mu). & & n_a = 2(\varkappa^{-1} - 1). \end{array}$$

The first belongs to the family of normal modes which is stable for all values of μ. The second family has a stationary a-state if $\mu = n_a^{-1} - 1$. If the static stability is greater than this value these modes are stable. If less, the modes are unstable. Let us consider the symmetric waves from each family in their evolution from a non-tilting state.

(i). $n^2 = -(2\mu + 1)$: From (15.3) we see that the symmetric resultant from this pair of modes has the a-state amplitude ratio $r_a = -1$. The field from the kinematic and dynamic vorticities are equal with opposite sign, so there is no perturbation of the basic flow in this a-state. As a consequence the temperature wave (the deformation of the boundaries) drifts passively downwind through the a-state with the air ($\dot{\sigma}_a = -1$). The vorticity wave on the other hand is driven downwind through the air by the overweight of the deformed boundaries. It moves downwind through the a-states as a simple neutral gravity wave with the intrinsic phase velocity μ (see 15.3). As the wave leaves the a-state the vorticity wave moves ahead of the temperature wave. The sliding vorticity maximum descends downwind from the interface crest and begins to grow and slow down. As the growing dynamic vorticity wave moves ahead of the kinematic vorticities the evolution of the temperature wave is dominated by the dynamic vorticity field because of its greater strength and more favorable tilt, so the temperature wave decays and moves downwind through the air with increasing speed as soon as it leaves the a-state. Both vorticity and temperature wave behaves in accordance with the rule in (15.7).

The temperature wave catches up with the vorticity wave again when both arrive together in the non-tilting b-state, the vorticity wave with maximum amplitude and minimum speed, the temperature wave with minimum amplitude and maximum speed. From (15.6) the vorticity wave moves through the b-state with the phase velocity

$$\dot{\theta}_b = -\frac{n^2}{\dot{\theta}_a} = -\frac{2\mu + 1}{\mu + 1}, \text{ or } \dot{\theta}_b + 1 = -\frac{\mu}{1 + \mu}.$$

The b-state amplitude ratio in (15.4) for this wave is therefore $r_b = -(\mu + 1)$, and from (15.5) its temperature wave moves downwind through the b-state with the maximum intrinsic phase velocity 2μ, driven by the dominating vorticity wave. The ratios between the amplitudes in the non-tilting states are obtained from (15.7). They are

$$(A_b/A_a)^2 = \dot{\theta}_a/\dot{\theta}_b = (\mu + 1)^2(2\mu + 1)^{-1}$$

$$(A_{sb}/A_{sa})^2 = \dot{\sigma}_a/\dot{\sigma}_b = (2\mu + 1)^{-1}.$$

The ratio of these gives $r_b/r_a = 1 + \mu$ which is the value we found earlier.

(ii). $n^2 = 1 - n_a(1 + \mu)$: From (15.3) the a-state amplitude ratio of the symmetric resultant of this pair of modes is $r_a = \mu$. The vorticity wave is stationary in this a-state and from (15.7) it remains stationary in this non-tilting state at all later times. The temperature wave moves through the a-state with the phase velocity $\dot{\sigma}_a = n_a(1 + \mu) - 1$. If $\mu = n_a^{-1} - 1$, this wave has a stationary neutral a-state. If the static stability is stronger, the temperature wave moves upwind through the a-state and the vorticity maximum which is left behind finds itself downwind from the interface crest where it decays. As the temperature wave moves upwind through the a-state it is augmented by the dynamic vorticity field and damped by the kinematic vorticity field. Which one of these two effects will dominate depends upon the relative strength of the fields in the a-state, that is the amplitude ratio $r_a = \mu$. For sufficiently strong static stability the dynamic vorticity fields dominate and the temperature wave grows as it moves upwind from the a-state. When it reaches the b-state the vorticity field which remained behind in the a-state has decayed to zero (see 15.4), so the temperature wave moves upwind through the b-state as the Rayleigh wave in the isentropic shear layer with the speed $\dot{\sigma}_b = n_b - 1 = 1$. If the static stability has the value of $\mu = 2n_a^{-1} - 1$, the temperature wave moves also through the a-state with unit speed. With this static stability the temperature wave of this $(n_b = 2)$-family is a neutral wave which moves upwind with the *constant* speed U while the dynamic vorticity field performs standing oscillations. With less static stability the kinematic vorticity field dominates and the temperature wave decays during its passage from the a-state to the b-state.

If the static stability is less than the value of $\mu = n_a^{-1} - 1$, the temperature wave moves downwind through the a-state and the stationary non-tilting sliding vorticity maximum is left behind in a position upwind from the interface crest where it is augmented by the overweight. The sliding vorticity field tends to dampen the temperature wave, but this effect is more than compensated by the dominating action of the kinematic vorticity field. So the entire wave grows when it has left the a-state. In the b-state the sliding vorticity is absent and the temperature wave moves upwind with the speed U. From either non-tilting state the wave therefore approaches the asymptotic state of the growing mode which from (14.5) and (15.1) has the stationary phase

$$\tan^2\theta_s = n^2 = 1 - n_a(1 + \mu). \qquad (n_b = 2)$$

From (12.5) the amplitude ratio in this mode is $r_s = \mu \cos \theta_s$.

In the unbounded isentropic shear layer this mode ($kd = 0.74$) is a little longer than the wave of maximum growth rate (see 6.9). Its growth rate is practically the same ($n = 0.55\ kU$), and its stationary phase is a little less downwind from the a-state ($\theta_s = 29°$). As the static stability across the interfaces is increased from zero it acts in two ways to reduce the growth rate of the mode: (i) It reduces the downwind tilt of the temperature wave and thus stops the kinematic vorticity field in a less favorable tilt for efficient growth of the deformations. (ii) The field from the dynamic vorticities reduces the growth still further.

For other wave lengths than $n_b = 2$ the physical wave mechanism is of course quite similar. However the symmetric waves from the two families of the normal modes have not the simple amplitude ratios in the non-tilting states, and their evolution can therefore not be described in detail before the numerical values of the roots n^2 of the frequency equation are known. The following qualitative remarks apply only to the unstable waves.

In the long unstable ($n_b > 2$)-waves the dynamic vorticity field of the growing mode has from (15.1) a state of stationary phase upwind from the a-state ($\theta_s > 0$), so the vorticity wave moves upwind through the a-state and downwind faster than the air through the b-state. From (15.3,4) the amplitude ratios in the non-tilting states of the unstable ($n_b > 2$)-waves must therefore obey the rules $r_a < \mu$, $r_b < 0$. Since the static stability is rather small in these long unstable waves ($\mu < n_a^{-1} - 1$), this means that the temperature wave moves downwind through the a-state a little slower than the same wave in the isentropic shear layer. It moves also slower upwind through the b-state than the corresponding isentropic wave due to its negative b-state vorticity. But the relative reduction of the speed is much less in the b-state. It is therefore clear that the growing mode of the ($n_b > 2$)-waves must be rather near the a-state with the vorticity wave tilting a little upwind and the temperature wave tilting less downwind than the corresponding isentropic Rayleigh wave ($\mu = 0$).

In the shorter growing ($n_b < 2$)-modes the stationary phase of the vorticity wave is downwind from the *a*-state with a smaller tilt than the temperature wave. In the symmetric waves of this unstable family the vorticity wave moves downwind through the a-state and upwind through the b-state, so the amplitude ratios are positive in both non-tilting states with $r_a > \mu$ and $r_b < \mu$. The temperature wave therefore moves slower downwind through the a-state and faster upwind through the b-state than the corresponding isentropic wave. The combined effect of these changes of the wave speed is to shift the stationary phase of the temperature wave upwind toward the a-state from the isentropic value ($\mu = 0$) for same wave length. The growing mode in the statically stable shear layer has always a smaller downwind tilt than the corresponding mode in the isentropic shear layer. For $n_b < 1$ the isentropic wave moves downwind through both non-tilting states and is therefore stable. However when the static stability is introduced in the layer ($\mu > 0$) the intrinsic upwind propagation of the corresponding symmetric temperature wave is augmented in both non-tilting states. For sufficiently strong static stability the wave will therefore move upwind through the b-state while still moving downwind in the a-state so the wave is unstable. This occurs for the range of static stabilities inside the unstable band. For still greater static stability the symmetric waves of the unstable family moves upwind through the a-states as well. So the waves are stable.

CHAPTER III

SHEAR LAYER WITH CONTINUOUS DISTRIBUTION OF STATIC STABILITY AND SHEAR

17. The statically stable Th-shear layer. We shall in this last chapter examine wave disturbances in a shear layer which resembles the discontinuous Taylor-Goldstein model in Chapter II, but which has continuous variation of the velocity and the potential temperature through the layer. The undisturbed flow has a hyperbolic tangent profile, namely

$$U = U_0 \,\mathrm{th}\,(2z/d). \tag{17.1}$$

We shall call this flow a Th-shear layer. Far from the center level the air moves in opposite directions with the same constant speed U_0. The air at the central level has the maximum shear $U'(z = 0) = 2U_0/d$. The parameter d in (17.1) may therefore be regarded as the depth of the most similar constant shear layer. The distribution of potential temperature in the layer is given by

$$\theta = \theta_0 \exp\,[2s\,\mathrm{th}^3(2z/d)]. \tag{17.2}$$

We shall assume that the total variation of potential temperature through the layer is a small fraction of the temperature at the central level, so the system is dynamically quasi-symmetric. With this assumption the potential temperatures far above and below the central level are approximately

$$\theta_w = \theta_0 e^{2s} = \theta_0(1 + 2s),$$
$$\theta_c = \theta_0 e^{-2s} = \theta_0(1 - 2s),$$

so the non-dimensional parameter s in (17.2) has the same meaning as in the discontinuous shear layer (see 2.2), namely

$$s = {}^1/_2(\theta_w - \theta_c)/(\theta_w + \theta_c) \ll 1. \tag{17.3}$$

In the following we shall use units of length and time such that $U_0 = {}^1/_2 d = 1$, and introduce the abbreviated notations.

$$T = \mathrm{th}\,(2z/d) = \mathrm{th}\,z$$
$$S = \mathrm{sech}\,(2z/d) = \mathrm{sech}\,z \qquad ({}^1/_2 d = 1)$$

These are connected by the useful relations

$$T' = S^2 = 1 - T^2,\; T'' = -2TT' = -2TS^2. \tag{17.4}$$

The static stability of the continuous stratification in (17.2) is represented by the logarithmic gradient of the potential temperature, namely

$$\sigma = (\ln\theta)' = 6sT^2S^2 \tag{17.5}$$

We note that this stratified Th-shear layer has maximum static stability and maximum change of the windshear at the levels

(17.6)
$$\sigma' = 0: \quad T^2 = {}^1/_2 \qquad (z = 0.43\, d)$$
$$T''' = 0: \quad T^2 = {}^1/_3 \qquad (z = 0.33\, d)$$

Both lie inside the boundaries of the "equivalent" constant shear layer ($z = {}^1/_2 d$). We must expect some difference between the dynamic properties of the continuous Th-shear layer and the "equivalent" discontinuous constant shear layer on this account.

18. The wave equations for the Th-shear layer. We now introduce into the Th-shear layer s amall amplitude disturbance such that the air parcels have the displacements $z_s(x,z)$ from their equilibrium levels and have the additional small amplitude motion

(18.1)
$$\boldsymbol{v}\,(x,z) = u\boldsymbol{i} + w\boldsymbol{k} = \nabla\psi \times \boldsymbol{j}.$$

Besides the vorticity of the basic flow the air has now the added vorticity of the disturbance, namely

(18.2)
$$q = -\nabla^2\psi = q_K + q_D.$$

As in the constant shear layer this added vorticity may be represented as a sum of two parts as indicated in (18.2) namely: (i) The kinematic vorticity q_k which comes from the advection of the vorticity U' of the basic flow due to the vertical displacements z_s of the air. (ii) The remaining part q_D which we call the dynamic vorticity. The advected kinematic vorticity has to the linear approximation the value

(18.3)
$$q_K = -U''z_s = 2TS^2 z_s.$$

The motion is isentropic so the potential temperature of the air particles is conserved. Associated with the vertical displacements of the air particles are therefore local changes in the potential temperature θ which, as in (18.3), to the linear approximation have the values

(18.4)
$$\bar{\theta} = -\theta' z_s = -\theta\sigma z_s.$$

The dynamic equation for the resultant motion, $\boldsymbol{V} = U\boldsymbol{i} + \boldsymbol{v}$, is

$$\frac{D\boldsymbol{V}}{Dt} = \boldsymbol{g} - (\theta + \bar{\theta})\nabla(\pi + \bar{\pi}). \qquad \pi = c_p \left(\frac{p}{100}\right)^{R/c_p}$$

We linearise this equation, then substitute the static pressure π from the static equation and eliminate the dynamic pressure $\bar{\pi}$ by $\nabla\,\boldsymbol{x}$ differentiation. The result, using (18.4) is

$$0 = \nabla \times \left[\theta^{-1}\left(\frac{D\boldsymbol{V}}{Dt} - \sigma g z_s \boldsymbol{k}\right)\right] \approx \nabla \times \left(\frac{D\boldsymbol{V}}{Dt} - \sigma g z_s \boldsymbol{k}\right).$$

The approximation to the right ignores the kinematic effect of the baroclinity. This is the quasi-symmetry approximation which is justified if the total temperature variation is a small fraction of the temperature; see for example FJØRTOFT [7]. With this approximation the dynamic equation takes the simple form

$$\frac{D}{Dt}(q + U') = \frac{Dq}{Dt} + wU'' = \sigma g \frac{\partial z_s}{\partial x}.$$

Separating out the kinematic vorticity q_K in (18.3), the equation gives the dynamic vorticity change

$$\frac{D}{Dt}(q - q_K) = \frac{Dq_D}{Dt} = \sigma g \frac{\partial z_s}{\partial x}.$$

The non-dimensional value of σg in units of $^1/_2 d = U_o = 1$, using (17.5), is

$$\sigma g = 6sgT^2S^2 = 3\mu T^2S^2. \qquad (\mu = sgd/U_o^2). \tag{18.5}$$

The non-dimensional form of the dynamic and kinematic equations for an arbitrary small amplitude disturbance of the Th-shear layer are therefore

$$\begin{aligned} &\frac{Dq_D}{Dt} = 3\mu T^2S^2 \frac{\partial z_s}{\partial x}, \qquad q_K = 2TS^2 z_s, \\ &\frac{Dz_s}{Dt} = \frac{\partial \psi}{\partial x}, \qquad -\nabla^2\psi = q_K + q_D. \end{aligned} \tag{18.6}$$

We shall use these equations to examine the behavior of wave disturbances which have a sinusoidal variation in the horizontal direction of the basic flow with an arbitrary non-dimensional wave number $k = {}^1/_2 kd$.

The stationary waves in an isentropic Th-shear layer were found by GARCÍA [8] in 1954. In 1961 GARCÍA investigated the Th-shear layer with the stratification in (17.2), and found all the possible stationary waves in this system. Although these results are not yet published, GARCÍA has kindly given me permission to refer to his solutions in this paper.

19. The non-tilting states of a wave in a Th-shear layer. As in (12.1) let r denote the amplitude ratio of the kinematic vorticity field to the kinematic vorticity field,

$$r = q_D/q_K; \qquad q = (1 + r)q_K. \tag{19.1}$$

In a non-tilting state the dynamic vorticity maximum is located at the crests of the deformed isotherms where the air particles have no overweight, so the wave is instantaneously neutral. Let $D(z)$ denote the instantaneous upwind intrinsic speed through the air of the dynamic vorticity wave in the non-tilting state, and let $C(z)$ denote the corresponding speed of the temperature wave. In frames which move locally with one of these waves, the wave has no local change, so from (18.6) we have

$$\frac{Dq_D}{Dt} = D\,\frac{\partial q_D}{\partial x} = 1.5\mu T\,\frac{\partial q_K}{\partial x},$$

$$\frac{Dz_s}{Dt} = C\,\frac{\partial z_s}{\partial x} = \frac{\partial \psi}{\partial x}.$$

With z_s represented in terms of the dynamic vorticity $q = (1 + r)q_K = 2(1 + r)TS^2 z_s$, these give the intrinsic phase velocities in the non-tilting states, namely

$$(19.2)\qquad \begin{aligned} D/U &= 1.5\mu/r, \\ C/U &= 2(1 + r)(S^2\psi/q). \end{aligned} \qquad (r = q_D/q_K).$$

These formulas resemble the corresponding phase velocity formulas in section 12 for the non-tilting states of the symmetric wave in a constant shear layer. In particular, we note that the pseed of the dynamic vorticity wave is determined entirely by the vorticity amplitude ratio. However, the wave in the Th-shear layer has 50% more dynamic vorticity than a wave with the same relative speed in the constant shear layer. The reason for this is at least partly that $U < U_0$ at all levels in the Th-shear layer, so the vorticity wave needs less overweight to have the same relative speed.

To predict the phase velocity of the temperature wave in (19.2) we must know both the amplitude ratio and the streamfunction of the wave. Inspection of the wave equations in (18.6) suggests that waves whose variation with height are simple functions of T and S may possibly have a simple analytical behavior. We therefore consider an initially non-tilting wave whose streamfunction has the form

$$\psi = A_n S^m T^n \cos kx,$$

where for the moment m and n are arbitrary non-negative constants. By substitution in (18.2) we find that the vorticity q associated with this field is given by

$$q/(S^2\psi) = (m + n)(m + n + 1) - n(n - 1)T^{-2} + (k^2 - m^2)/S^2.$$

We shall in the following only consider waves of this type for which $m = k$, so the last term on the right is zero. Introducing the abbreviation

$$(19.3)\qquad K_n = (k + n)(k + n + 1),$$

these waves have the wave elements

$$(19.4)\qquad \begin{aligned} \psi_n &= A_n T^n S^k \cos kx, \\ q_n &= A_n[K_n T^n - n(n - 1)T^{n-2}]S^{k+2} \cos kx. \end{aligned}$$

By substitution in (19.2) we see that the instantaneous relative phase velocities of the $(n = o)$-wave and the $(n = 1)$-wave are independent of height if the amplitude ratio is a constant. Let us examine these two waves a little further.

20. The non-tilting a-wave ($n = 1$). The streamfunction and vorticity of this wave are

$$\psi = TS^k \cos kx, \qquad q/(S^2\psi) = K_1. \tag{20.1}$$

The wave has a nodal plane at the central level with symmetric fields in opposite phase above and below, so it resembles the non-tilting a-state of the symmetric wave in the constant shear layer. From (19.2) the dynamic vorticity wave and the temperature wave moves upwind with the relative intrinsic phase speeds

$$D/U = 1.5\mu/r; \qquad C/U = 2(1 + r)/K_1. \tag{20.2}$$

The wave is a stationary neutral wave ($D = C = U$) if the amplitude ratio has the value $r = 1.5\mu$ and the parameter K_1 in (19.3) has the value

$$K_1 = 3\mu + 2 = (k + 1)(k + 2). \qquad (D = C = U). \tag{20.3}$$

This is one of the families of stationary solutions which were found by García (see section 22 below).

To compare these stationary a-waves with the stationary a-waves in the constant shear layer we recall that $k = {}^1/_2 kd = {}^1/_2 \varkappa$, so the stationary wave condition in (20.3) may be written

$$3\mu = {}^1/_4 \varkappa^2 + 3({}^1/_2 \varkappa). \qquad (\varkappa = kd). \tag{20.4}$$

In the $\varkappa,\mu$-diagram (see fig. 21) this parabola coincides near the origin, to the order of $\varkappa^2$, with GOLDSTEIN's a-line for the stationary a-waves in the constant shear layer between unbounded outer layers (see 12.8). For the shorter waves the parabola in (20.4) lies above the Goldstein-line. The stationary a-wave of $\varkappa = 1$ in the constant shear layer has the static stability $\mu = (e - 1)^{-1} = 0.582$. The same wave in the Th-shear layer has the static stability $\mu = 7/12 = 0.584$. The stationary a-wave parabola for the Th-shear layer is practically coincident with the stationary a-wave line for the constant shear layer for all waves longer than $2\pi d$. This remarkable coincidence suggests that the two systems have similar dynamic characteristics for waves which are much longer than the depth of the shear layer. However there are significant differences between the two systems which become evident when we consider the a-waves in (20.1), for wave lengths other than the stationary waves. If the amplitude ratio is $r = 1.5\mu$, the vorticity wave is stationary. The temperature wave moves upwind through the a-state if the wave is longer than the stationary wave, and downwind if it is shorter. This agrees qualitatively with the behavior of the waves in the constant shear layer. However the phase velocities are different in the two systems. In the constant shear layer the temperature wave moves through the a-state with the intrinsic phase velocity in (12.7) which with present notations may be written

$$C/U = n_a(1 + r). \qquad n_a = (1 - e^{-\varkappa})/\varkappa.$$

The temperature wave is moved through the air partly by the field from the dynamic vorticities and partly by the kinematic vorticities. In absence of the dynamic vorticity field ($r = 0$) the temperature wave would move through the a-state with the intrinsic speed;

Constant shear layer: $C_a/U = (1 - e^{-\varkappa})/\varkappa.$ $(\to 1 - {}^1/_2\varkappa).$

Th-shear layer: $C_a/U = (1 + {}^3/_4\varkappa + \varkappa^2/_8)^{-1}.$ $(\to 1 - {}^3/_4\varkappa).$

Both have the same asymptotic value $C_a = U$ for the very long waves, but the departure from the asymptote is 50% greater in the Th-shear layer.

21. The non-tilting b-wave ($n = 0$). — From (19.4) the streamfunction and vorticity of this wave is

(21.1) $$\psi = S^k \sin kx, \qquad q = k(k+1)S^2\psi$$

The wave is symmetric with respect to the central level with the same phase above and below, so it is of the b-wave type. Its instantaneous relative phase velocities (19.2) are

$$D/U = 1.5\mu/r, \qquad C/U = 2(1 + r)/K_o.$$

This wave is a stationary neutral wave if its amplitude ratio is $r = 1.5\mu$ and the parameter K_o (see 19.3) has the value

(21.2) $$K_o = 3\mu + 2 = k(k+1). \qquad (D = C = U).$$

The corresponding $\varkappa,\mu$-parabola,

$$3\mu = {}^1/_4\varkappa^2 + {}^1/_2\varkappa - 2, \qquad (\varkappa = kd).$$

is very different from the line for the stationary b-wave in the constant shear layer (see 12.8 and fig. 21). The reason for this is that the wave in (21.1) has the maximum vorticity near the central level where the wave in the constant shear layer has no added vorticity. The partial field from the vorticity in the central region augments the upwind propagation of the temperature wave at all levels, so the stationary wave in (21.1) is shorter than the stationary b-wave in the constant shear layer. If the excess vorticity in the central region is removed from the wave, the temperature wave would move downwind at all levels, similar to the same wave in the constant shear layer.

It is impossible to set up a stationary b-wave in the Th-shear layer unless it is given excess vorticity near the central level, where no such vorticities can be generated by kinematic advection or by dynamic action of the overweight. However, with the aid of the field of the a-wave in (20.1) we may construct a b-wave which has no excess vorticity at the central level simply by changing the sign of the a-wave vorticity in the lower layer. Accordingly this b-wave has the vorticity field

(21.3) $$q = K_1 |T| S^{k+2} \cos kx.$$

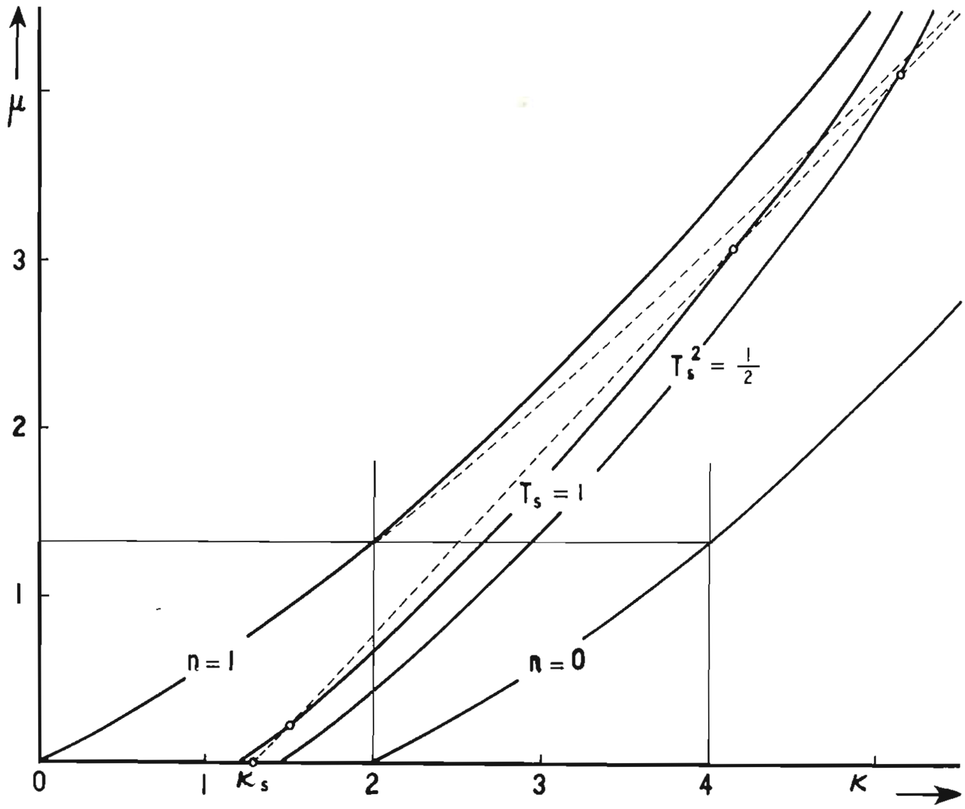

Fig. 21: Stationary waves in a Th-shear layer.

Above the central level this wave has the same vorticity as the a-wave in (20.1). The partial field from the vorticities below the central level is Laplacean in the upper region for both waves, so the two waves differ only by a Laplacean field. Above the central level the stream-function of the vorticity wave in (21.3) accordingly has the form

$$\psi = (TS^k + Ae^{-kz}) \cos kx. \qquad (z > 0)$$

Since the field is symmetric with respect to the central level we have $\psi'(z = 0) = 0$, so $A = k^{-1}$. The streamfunction of the vorticity wave (21.3) is therefore

$$\psi = (|T| S^k + k^{-1}e^{-k|z|}) \cos kx. \tag{21.4}$$

If this wave has the amplitude ratio $r = 1.5\mu$, the dynamic vorticity wave is stationary, and from (19.2) the temperature wave in the upper region has the relative speed

$$\frac{C}{U} = \frac{3\mu + 2}{(k+1)(k+2)} \left(1 + \frac{1}{kT(1+T)^k}\right) \qquad (r = 1.5\mu). \tag{21.5}$$

Its upwind speed is greater than in the corresponding a-wave (20.2). For very short wave lengths it has the same asymptotic behavior as the a-wave. In particular the condition for a stationary short wave is the same (20.3) for both waves. For the longer b-waves in (21.4), on the other hand, the relative speed of the temperature field is a function of height, so for no value of the static stability are these waves stationary at all levels simultaneously. The wave is stationary at a given level $z = z(T_s)$ if the static stability has the value of

$$3\mu + 2 = (k+1)(k+2)\left(1 + \frac{1}{kT_s(1+T_s)^k}\right)^{-1}, \qquad C(T_s) = U. \tag{21.6}$$

At higher levels this wave moves slower than the air, at lower levels faster. The wave is stationary far from the central level if

$$3\mu + 2 = (k+1)(k+2)[1 + (k2^k)^{-1}]^{-1}. \qquad C(T_s = 1) = U_o$$

This line is shown in the $\mu,\varkappa$-diagram in fig. 21. It meets the Goldstein line for the stationary b-waves in the constant shear layer at $\varkappa = 2k = 1.5$ and at $\varkappa = 4.15$. In the spectral interval between these waves the stationary b-wave in the constant shear layer has a little more static stability. For example the $(\varkappa = 2)$-wave in the constant shear layer is stationary if $\mu = (e^2 - 1)/(e^2 + 1) = 0.76$, while the same wave in (21.4) is stationary far from the central level if $\mu = 2/3$.

We recall from (17.6) that the Th-shear layer has maximum static stability at the level of $T^2 = {}^1/_2$. With this value of T_s substituted, equation (21.6) marks the waves in (21.4) which are stationary at the level of maximum stability. The corresponding line is shown in fig. 21. These waves have considerably less static stability than the stationary b-waves in the constant shear layer. The main reason is probably that the vorticity field in (21.3) has a unrealistically large value near the center level where there is no physical mechanism for the generation of vorticity.

Let us therefore consider a third class of b-waves which has very little vorticity near the central level, namely waves with the vorticity distribution $q \sim T^2S^k$. The stream function of this wave is obtained by taking the resultant of two of the waves in (19.4). Omitting the trigonometric factor, the waves of $n = 0$, and $n = 2$ are

$$q_o = K_oS^{k+2}; \qquad \psi_o = S^k$$

$$q_2 = (K_2T^2 - 2)S^{k+2}; \qquad \psi_2 = T^2S^k.$$

The resultant of these, augmented by the proper factors, is

$$q = K_oK_2T^2S^{k+2}; \qquad \psi = (2 + K_oT^2)S^k. \tag{21.7}$$

If the amplitude ratio of this wave is $r = 1.5\mu$, its dynamic vorticity wave is stationary and its temperature wave moves with the intrinsic upwind speed

$$\frac{C}{U} = \frac{3\mu + 2}{(k+2)(k+3)}\left(1 + \frac{2}{k(k+1)T^2}\right). \qquad (r = 1.5\mu). \tag{21.8}$$

This wave has maximum vorticity at the levels of $T^2 = {}^1/_2(1 + {}^1/_4k)^{-1}$. For the very long waves these coincide with the levels of maximum stability (see 17.6). For $k = 2$ they coincide with the levels of maximum gradient of the wind shear. For $k = 0.8$ the levels of maximum vorticity are in the middle between the levels of maximum stability and maximum wind shear gradient. The wave in (21.7) is stationary at the level of maximum stability ($T^2 = {}^1/_2$) if the stability has the value of

(21.9) $$3\mu + 2 = \frac{k(k+1)(k+2)(k+3)}{k^2+k+4}. \qquad C(T^2 = {}^1/_2) = U.$$

In a $\mu,\varkappa$-diagram ($\varkappa = 2k$) this line meets the line for the stationary b-wave in the constant shear layer at the points ($\mu = 0$, $\varkappa = \varkappa_s = 1.278$ . .) and ($\mu = 1.75$, $\varkappa = 2.9$). Between these points the wave in (21.9) has a little less static stability, but otherwise its properties are quite similar to those of the stationary b-wave in the constant shear layer. Like the stationary a-waves in section 20 this similarity probably reflects a fundamental dynamic similarity between the Th-shear layer and the constant shear layer. However, whereas the constant shear layer has only these two families of stationary waves, the Th-shear layer has an infinite number of such families.

22. The stationary waves in the Th-shear layer. (García's solutions). From (19.2) the general condition for a stationary wave in the Th-shear layer with reference to the fluid at the central level ($D = U = C$) is

(22.1) $$q = -\nabla^2\psi = \nu S^2\psi. \qquad (\nu = 3\mu + 2).$$

When the streamfunction has a sinusoidal variation in the x-direction, García noticed that this differential equation, by suitable transformation, is the hyper-geometric differential equation. As such its solutions may be represented by the series

(22.2) $$\psi = \sum_{m=o}^{m=n} A_m T^m S^k \cos kx,$$

where the coefficients A_m are the coefficients of the hyper-geometric series. These coeffisients are in the present case easily determined by the formulas in (19.4): The field in (22.2) has the vorticity

(22.3) $$q = \sum_{m=o}^{m=n} A_m[K_m T^m - m(m-1)T^{m-2}]S^{k+2} \cos kx.$$

With these substituted in the stationary wave equation (22.1) the coefficient for T^m gives

$$A_m(K_m - \nu) + (m+1)(m+2)A_{m+2} = 0.$$

Repeated use of this recursion formula gives

(22.4) $$A_m = A_o(\nu - K_o)(\nu - K_2) \ldots (\nu - K_{m-2})(m!)^{-1} \qquad (m \text{ even})$$

(22.5) $$A_m = A_1(\nu - K_1)(\nu - K_3) \ldots (\nu - K_{m-2})(m!)^{-1} \qquad (m \text{ odd})$$

Thus ψ in (22.2) is a solution of the differential equation if

$$\nu = K_n, \text{ or } 3\mu + 2 = (k + n)(k + n + 1), \tag{22.6}$$

where n is any non-negative integer. If n is an even integer, $A_1 = 0$ and the coefficients A_m have the values in (22.4). If n is an odd integer, $A_o = 0$ and the coefficients A_m have the values in (22.5).

The stationary wave conditions in (22.6) are represented in the k,μ-diagram by a family of identical parabolas, each displaced unit distance toward decreasing k from the next lower member. The $(n = 0)$-parabola marks the stationary b-waves (see 21.2) which have no nodal plane. The $(n = 1)$-parabola marks the stationary a-waves (see 20.3) which have one nodal plane at the central level. The n^{th} parabola marks the family of stationary waves with n nodal planes. If n is odd the central level is a nodal plane and the field has opposite phase at equal heights above and below. The wave is of the a-type. If n is even, the wave has the same phase and amplitude at equal heights above and below the interface. The wave is of the b-type.

By examining all the solutions of the hyper-geometric equation García found that the solutions in (22.6) represent all the stationary waves in the Th-shear layer with the stratification (17.2) which have bounded and continuous velocity fields.

REFERENCES

1. Taylor, G. I., 1931: Effect of Variation in Density on the Stability of Superposed Streams of Fluid. *Proc. Roy. Soc.* A **132**, pp. 499–523.
2. Goldstein, S., 1931: On the Stability of Superposed Streams of Fluids of Different Densities. *Proc. Roy. Soc.* A **132**, pp. 524–548.
3. Høiland, E., 1948: Stability and Instability Waves in Sliding Layers with Internal Stability. *Arch. Math. og Nat.* L. Nr. 3.
4. Lord Rayleigh, 1880: On the Stability and Instability of Certain Fluid Motions I. *Scientific Papers.* Article 66. Vol. I, p. 474.
5. Kirchhoff: *Mechanics* XX; Lamb, *Hydrodynamics.* p. 232.
6. Chandrasekhar, S., 1953: *Proc. Roy. Soc.* A **217**, p. 306.
7. Fjørtoft, R., 1950: Applications of integral theorems etc. Chapter III. *Geof. Publ.* XVII, N° 6.
8. García, R. V., 1956: Barotropic Waves in Straight Parallel Flow with Curved Velocity Profile. *Tellus,* **8**, pp. 82–93.

(Manuscript received 14 August 1961)